2005

Long term pressure behavior in turbidite reservoirs

Feng Wang
Louisiana State University and Agricultural and Mechanical College, fwang1@lsu.edu

LONG TERM PRESSURE BEHAVIOR IN TURBIDITE RESERVOIRS

A Dissertation

Submitted to the Graduate Faculty of the
Louisiana State University and
Agricultural and Mechanical College
in partial fulfillment of the
requirements for the degree of
Doctor of Philosophy

in

The Department of Petroleum Engineering

by
Feng Wang
B.S., University of Petroleum (East China), 1993
M.S., Louisiana State University, 2001
May 2005

ACKNOWLEDGEMENTS

The author expresses his sincere thanks to Dr. Christopher White for his enlightenment, guidance, patience and encouragement. His insights and suggestions have always been valuable and beneficial during the course of this research. The author owes a lot to him.

This project was funded by Shell Exploration & Production Company. Without their support, this work would not have been possible.

Thanks to Dr. Zaki Bassiouni, Dr. Andrew Wojtanowicz and Dr. Julius Langlinais in the Department of Petroleum Engineering and Dr. Barb Dutrow in the Department of Geology and Geophysics who were enthusiastic to serve on the examining committee and gave valuable suggestions.

Thanks to my wife, Shaohua Wang, who have made my life much more colorful and gave me encouragements during some difficult periods. Without her spiritual support, this work would not have been completed.

Thanks extend to all other faculty members and students who have offered help and been kind to the author and made the past several years enjoyable and memorable.

TABLE OF CONTENTS

LIST OF TABLES

LIST OF FIGURES

ABSTRACT

In this study, we investigated several possible mechanisms that would give rise to the anomalous pressure behavior (early concave-up on Horner plot or upward drift on the derivative curve of the log-log plot and asymmetry between the pressure drawdown and buildup behavior) sometimes encountered in the turbidite reservoirs in GOM primarily using numerical simulation and 2-level experimental designs. We ascertained the most influential parameters to the pressure behavior and identified that multilayer commingled system and the leaky compartment model are the most probable mechanisms to cause the anomalous behavior due to layer or zone property contrast to a certain degree. Differential depletion was found to be the main reason for the asymmetry between the pressure drawdown and buildup. Distinctive drawdown and buildup pressure behavior and numerical convolution and deconvolution were tried to obtain influence functions for discriminating the two systems.

The multilayered system was further investigated quantitatively by a three-layer model representing low, medium and high properties of a reservoir using a 3-level experimental design and the response surface method. The response is the shape of the derivative curve corresponding to each combination of reservoir parameters, which is represented by the coefficients of the polynomial obtained by non-linear piecewise regression. Significant influential reservoir parameters were identified by their influence upon the shape of derivative curves when their value changed. In addition, if we have the actual pressure data obtained from well testing, we can obtain parameter value estimates by matching the derivative curve plotted from actual pressure data using the response surface models (only contains significant factors) that describe the relationship between

the derivative curve shape and the factors. We may need correlate with other data source such as well logging data to verify the parameter estimates.

CHAPTER 1. INTRODUCTION

Significant oil and gas reserves occur in layered turbidite reservoirs. Turbidites are the primary reservoir type in deep water. With the global exploration and development increasingly going to deep water, turbidites are a primary target. More oil and gas may be produced from the turbidites in the future because turbidite exploration and production are still at an immature stage. This trend has been reinforced by deep water drilling in Brazil, North Sea, the Gulf of Mexico and the West Africa (Pettingill et al., 1998). Although the depositional origins of these reservoirs are still subject to some controversy – they are variously interpreted as channel-levee, lobe, and channelized deposits – their layered nature is clear in wireline logs and core samples (**Figure 1**). Often, the turbidite reservoirs are thin-bedded, on the order of centimeters or even millimeters. Examples in the Gulf of Mexico include the Tahoe M4.1 sand, the Ram-Powell L sand, and the Glider G-sands. A complete or incomplete sequence or cycle is often present in the turbidites. Graded bedding is generally a characteristic of turbidite deposits. However, the fine-grained deposits commonly encountered in the U.S. Gulf of Mexico may have such a narrow grain size range that graded bedding will never be observable (Bouma, 2001).

In well testing terminology, turbidite reservoir formations can be treated as multilayered systems. Each layer may have different thickness, permeability, porosity, and skin factor. The layer flow capacity (kh) and storage capacities (ϕhc_t) may differ significantly, leading to differential pressure depletion between the layers.

If the layers are not entirely separated by impervious layers and communicate vertically, then interlayer crossflow occurs, which affects all intercommunicating layers. When the transient layer interaction stabilizes, the response of the layered formation is

similar to a uniform formation with composite flow properties of the individual layer (Streltsova, 1988).

If the layers are separated by impermeable barriers such as shale and communicate only through the wellbore, then the production is said to be commingled. The well may never reach a regime in which its pressure-rate behavior can be approximated with averaged flow and storage capacities. In general, reservoirs consist of some crossflow zones and some commingled zones, which makes the situation more complex.

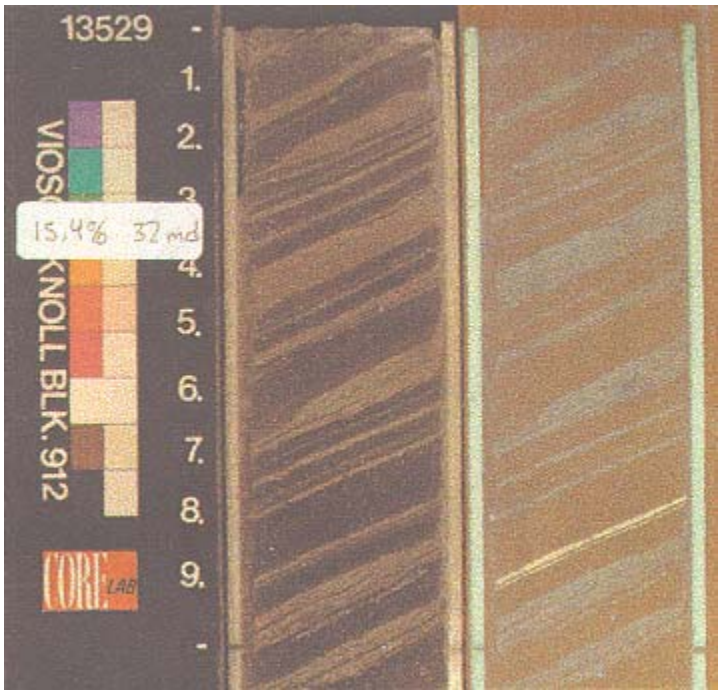

Figure 1. Core taken from Ram Powell L Sand

The VK912-2 core is taken from the thickest, proximal part of the eastern levee of the Ram Powell L sand. The main characteristic of this core is its laminated appearance (Bramlett and Craig, 2002).

Within each layer, areal heterogeneity may also be significant. A reservoir may have areas with distinctly different properties laterally so that the reservoir is compartmentalized. Commonly, a reservoir is terminated by permeability variations such

as stratigraphic pinchouts and faults in one or more directions, giving the reservoir a complex shape in three dimensions. Reservoir properties (permeability, porosity and thickness) have to be treated as functions of reservoir locations in these cases.

The pressure behavior is not only influenced by reservoir characteristics, but also influenced by wellbore conditions. If the well is opened and shut in on the surface, then wellbore storage effects due to fluid compressibility can mask the early pressure transient behavior. Moreover, wellbore conditions like partial perforation, hydraulic fracturing and phase segregation also influence pressure responses significantly.

In addition, typical deepwater Gulf of Mexico reservoirs are unconsolidated to slightly consolidated Miocene-, Pliocene-, and Pleistocene-age turbidite sands. Such sands may be prone to considerable compaction for large pressure drawdowns (several thousand psi) during the production of the reservoir (Ostermeier, 2001). Compaction affects permeability strongly, which can impair reservoir productivity. On a relative basis, compaction reduces permeability four to five times more than it reduces porosity (Ostermeier, 2001).

Besides the complexity of the layered turbidite reservoirs and wellbore conditions, problematic pressure gauge performance caused by harsh borehole environment and gauge/electronic characteristics may cause noise, loss of precision and systematic errors in pressure records. Gauge problems can be misinterpreted as reservoir effects (Kikani and others, 1995). Flow rate measurement error and uncertainties in model recognition, parameter estimation and fluid and rock properties also reduce confidence in the well test interpretation (Horne, 1994). Moreover, flow history of a well has pronounced influence on the drawdown pressure behavior. Approximating variable rate by a constant rate, as

often practiced in well test analysis, may cause significant errors in parameter estimations.

In practice, a multilayer reservoir is often simplified to a single-layer reservoir for well test interpretation due to the difficulty of parameter specification and production rate allocation to each layer. Multilayer effects are thus averaged over the whole reservoir. This averaging is not generally consistent with the true situation of the multilayered reservoir because of factors such as crossflow, skin variation, compaction and permeability anisotropy and heterogeneity.

CHAPTER 2. PROBLEM STATEMENT AND PROPOSED APPROACH

2.1 Background and History

The pressure transient and production behavior of layered turbidites has proved to be complex and difficult to predict. Well tests in the turbidite reservoirs share several important features. Initial production tests were often anomalous. In the case of the Ram-Powell L Sand, there was a pronounced concave-upward shape on the Horner plot and there was rapid upward drift that began at very early time on the derivative curve of the log-log plot (Ram-Powell Well A2 in **Figure 2**).

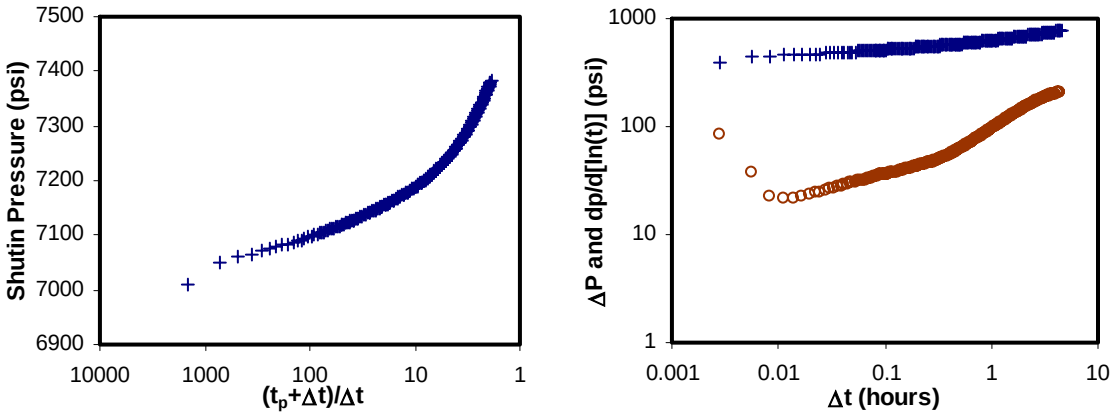

Figure 2. Horner and log-log plot of Well A2 in Ram Powell Field

The data were taken from permanent gauge pressure data of Ram-Powell A2, which are buildup data from 10:43 to 15:20 1/29/1998. There was 4 hours production before shutin. There is an evident concave-up shape in the Horner plot (left graph) and a rapid upward drift in the derivative on the log-log plot (right graph). There are no models which can match both the early-time and late-time behavior satisfactorily. This kind of pressure response anomaly has been widely observed in Gulf of Mexico turbidite reservoirs.

It was difficult to find models that matched both early-time and late-time behavior, although the late data seemed to be consistent with pressure support from a poorly-connected region. At Tahoe, the early production test response was surprisingly ideal (Tahoe Well A3 in **Figure 3**), indicating an apparently uniform reservoir despite the heterogeneous sand-shale succession observed in cores and wireline logs; no barriers

("leaky" or total) were detected (White and others, 1992). The later production response of Tahoe has been more complex: as depletion continued, the concave-up shape observed at Ram-Powell began to dominate Tahoe pressure response as observed in permanent down-hole gauges (Tahoe Well SE in **Figure 4**). The early-time features of pressure response are especially distinct from that of early production. In particular, the drawdown and buildup behavior of these systems are different, with the drawdown response being more "normal" and the buildups exhibiting the pronounced concave-upward "signature" of the anomalous response in these layered turbidite reservoirs.

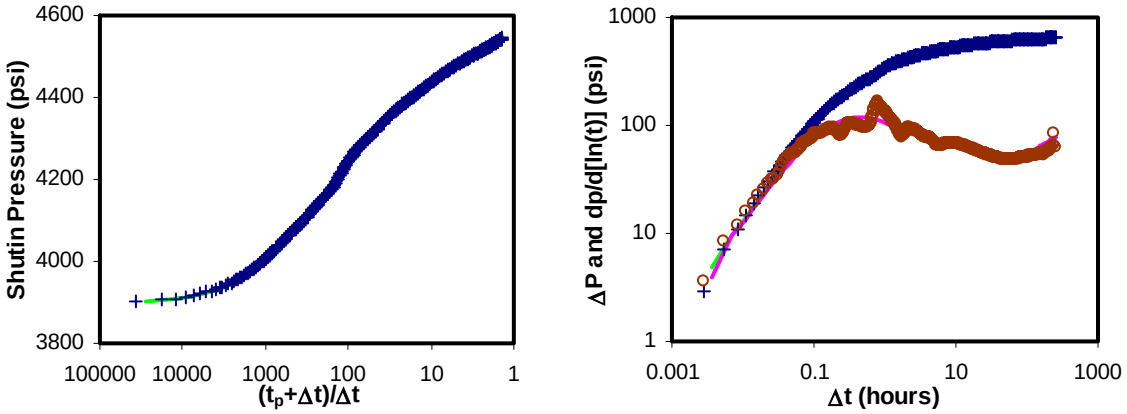

Figure 3. Horner and log-log plot of Well A3 in Tahoe Field

The data were taken from permanent gauge pressure data of Tahoe A3, which are buildup data from 5:26 9/6/1997 to 0:00 9/17/1997. There was about 170 hours' production before shutin. This pressure response occurred at the early production stage, about two months after the initial production. Both the Horner plot (left graph) and log-log plot (right graph) indicate a uniform reservoir. A model matched the data almost perfectly.

2.2 Proposed Mechanisms

A variety of mechanisms including Leaky-compartment and U-shaped faults have been proposed to explain the anomalous pressure behavior. However, these explanations are unsatisfactory.

- None of these models adequately match our expectations of reservoir rock properties and geologic setting, such as faults, layering, and lateral continuity.
- No currently available model matches the pressure and rate responses over the full range of observations, including initial tests and long-term production behavior.

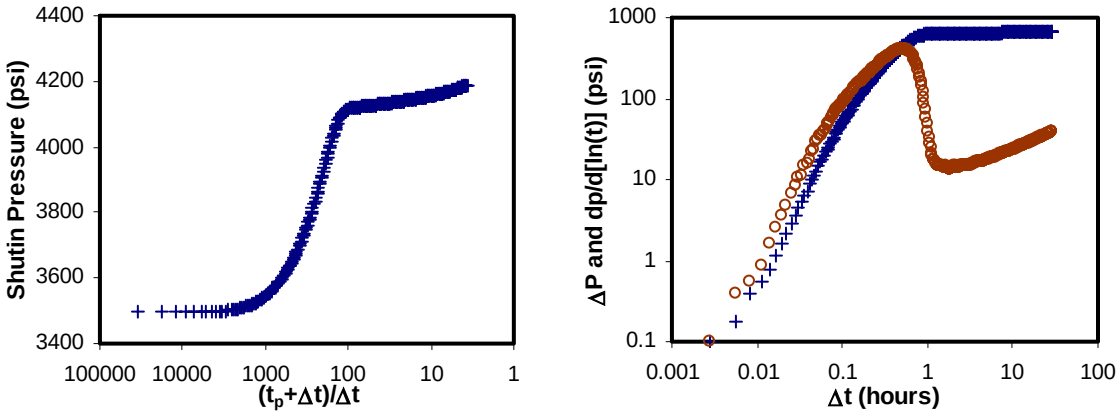

Figure 4. Horner and log-log plot of Well SE in Tahoe Field

The data were taken from permanent gauge pressure data of Tahoe SE, they record a buildup from 16:00 2/16/1998 to 12:24 2/21/1998. There was about 100 hours production before shutin. For the log-log plot (right graph), there is an obvious early-time concave-up trend in the Horner plot (left graph).

There are several shared features in these responses that give clues of its possible causes. The time at which these features are first observed suggests that depletion is an important factor in initiating the response. Differential depletion may cause a non-uniform flux distribution during production, and possibly causes significant wellbore crossflow during buildup tests. Clear identification and correct analysis of these behaviors will requires examination of reservoir geometry, rock properties, and well characteristics. Differential depletion, permeability heterogeneity, horizontal and vertical flow baffles, skin varying by layer, and rate history could interact to cause these complex responses.

Pressure response, productivity, and recovery efficiency are linked in oil and gas reservoirs. The current incomplete understanding of the pressure behavior of these systems makes it difficult to derive material balance models with confidence or to build accurate reservoir models to forecast production.

2.3 Factors Investigated

In this research program, we investigate layered turbidite reservoir behavior using analytic and numerical models. An extended and thorough investigation is required because considerable effort has already been devoted to this problem without yielding adequate methods to analyze and predict pressure transient, material balance and recovery behavior of layered turbidite reservoirs. Features to be studied will include:

- vertical and lateral changes in permeability of sand layers;
- vertical transmissibility variations caused by areal variations, amalgamation, sand quality, sand thickness, and net-to-gross;
- Lateral transmissibility variations due to faults, lithologic changes, and stratigraphic changes;
- wellbore models, including differing layer skin effects and near-wellbore compaction as possible causes of the asymmetry in drawdown and buildup behavior.

Compared to analytic models, numerical models allow more flexibility. Analytic solutions only exist for some ideal reservoir and boundary conditions. Sometimes even the analytic solutions have to be approximated by simpler function forms or by numerical calculation. For example, analytic pressure transient solutions with wellbore storage and skin are obtained in Laplace space, cannot be inverted to real time analytically, and so are

commonly evaluated using an accurate and robust but approximate inversion scheme (Tariq and Ramey, 1978, Stehfest, 1970). Layered reservoir solutions are yet more trenchant, involving extraction of eigenvalues in Laplace space and approximate numerical inversion. In the end, these methods are no faster or more reliable than a carefully prepared numerical simulation model. Moreover, numerical models can represent irregular reservoir geometry, reservoir heterogeneity, complex inner and outer boundary conditions, and multiphase fluid properties. Therefore, numerical models will be emphasized in the modeling phase of this study. However, analytical solutions will also be investigated due to their explicit mathematical expressions and feasibility, and will be used to guide interpretation of models and field measurements.

Many factors influence pressure response. Sensitivity analysis on these factors will focus this study on factors that most affect pressure response. Experimental designs will be used for the sensitivity analysis. Instead of changing factors one-at-a-time, by which factor interactions cannot be obtained and a large number of simulation runs is needed, factors are changed systematically in experimental design to reveal effects and interactions using a smaller set of designed simulation runs (Box and Draper, 1987). We will create numerical models sequentially, progressing from simple to more complex models.

CHAPTER 3. POSSIBLE MECHANISMS

3.1 U-Shaped Impermeable Boundary Model

The concave-up shape on the Horner plot often leads us to the U-Shaped impermeable boundary model. In this model, a single well is located at some distances from three impermeable boundaries, two of which are parallel and intersected by the third at a right angle (**Figure 5**). Using the method of images and superposition in space, we can obtain the bottom hole pressure of the well for pressure drawdown. For pressure buildup, we also need superposition in time. For the U-shaped boundaries, an infinite number of image wells are required in principle. In practice, the distant image wells have negligible effects and it will take longer time for the more distant image wells to be felt at the real well. Depending on the location of the well, after the early-time infinite acting period, the pressure trend may first indicate a single impermeable boundary, possibly followed by the effects of two mutually perpendicular or two parallel boundaries, then finally exhibiting the characteristics of the three influencing no-flow boundaries (Streltsova, 1988).

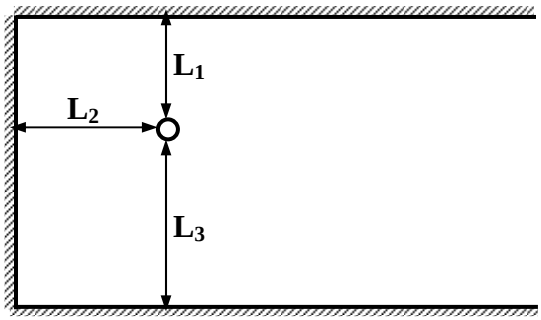

Figure 5. Schematic diagram for U-shaped boundary model

To illustrate the influence of U-shaped boundaries, we designed 4 cases for different well locations by changing the distances from the well to the three boundaries. The basic parameters for the reservoir are listed in **Table 1**, which we will use throughout

this study. We run the simulations and plot the pressure difference and pressure derivative curves (**Figure 6**). We can clearly see from the log-log plots that the pressure derivative curves are rather distinct and sensitive for different well locations. For the derivative curve to be concave-up at early time, the no-flow boundaries would have to be very close to the well. However, there is little evidence that the wells in which similar behavior has been observed are in fact close to faults or other quasi-linear barriers.

Table 1. Basic Parameters for Reservoir Models in This Study

Porosity	**Compressibility** 1/psi	**Formation Volume Factor** rb/stb	**Viscosity** cp
0.3	7×10^{-5}	0.98	4

3.2 Leaky-compartment Model

Increasing evidence for reservoir heterogeneity with compartmentalized geometry has been witnessed in recent decades (Junkin and others, 1992). Anomalous well tests are often attributed to the leaky-compartment model. This model treats the reservoir as a collection of tank-like chambers with leaky barriers allowing a certain degree of communication between them. Here we use a radial model with an outer zone and an inner zone to approximate the compartments. The outer zone and the inner zone have different permeability and a barrier between them. This kind of compartmentalized behavior becomes prominent in the pressure history at late times when the other connected compartments start contributing (Rahman and Ambastha, 1996). By adjusting the pore volume of the two zones and the transmissibility of the barrier, we can obtain

different pressure responses. Again we use reservoir simulation to realize this, for simplicity and consistency, although analytic solutions are available (Fox and others, 1988, Stewart and Whaballa, 1989, Rahman and Ambastha, 1997)

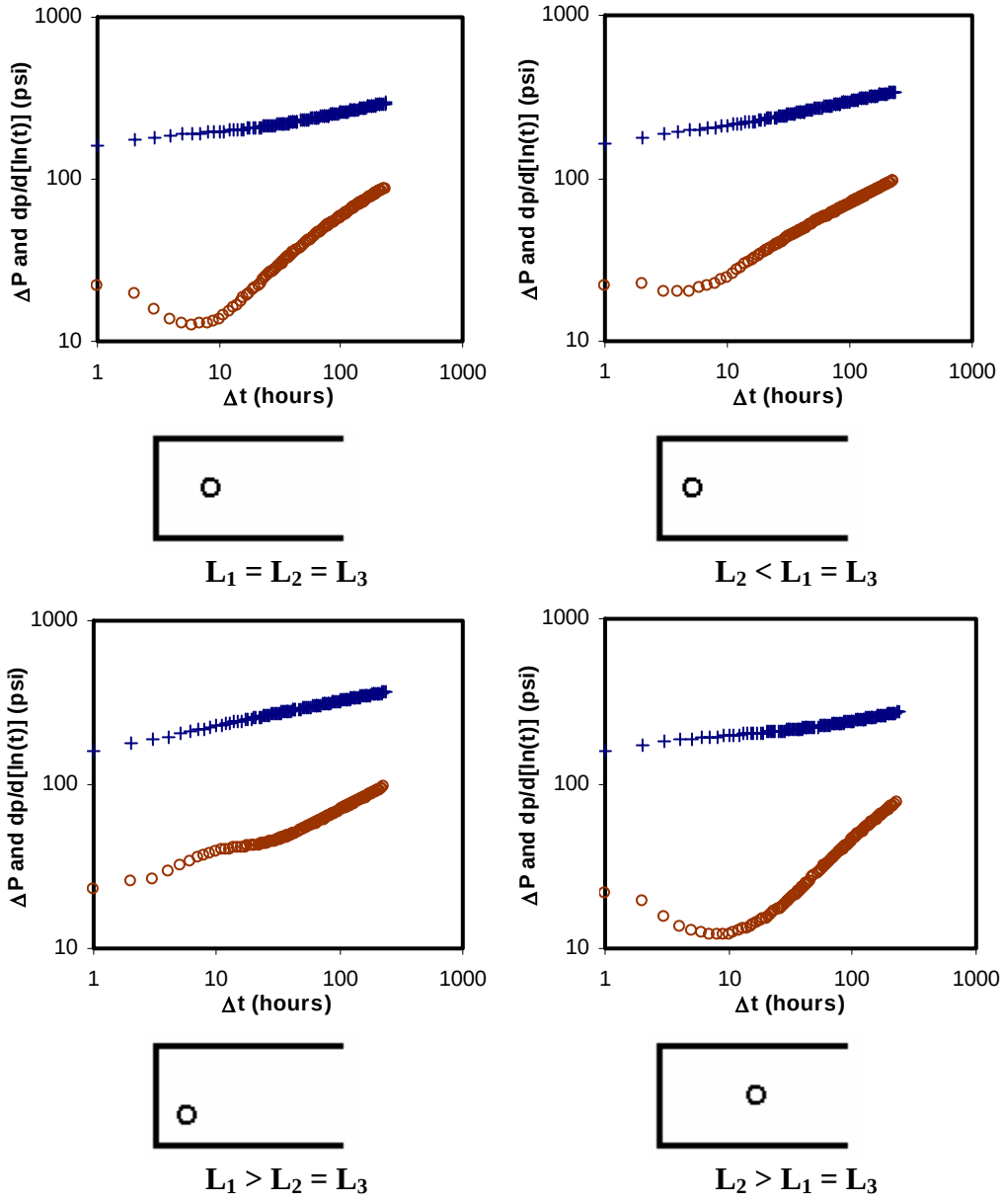

Figure 6. Log-log plots for different well locations for U-shaped boundary model

We make a simple 2^2 factorial design according to the design factors and design levels shown in **Table 2**. Permeability is fixed for the two zones, 1000 md for inner zone

and 10 md for outer zone. The factors considered in the design are pore volume and transmissibility between the two zones.

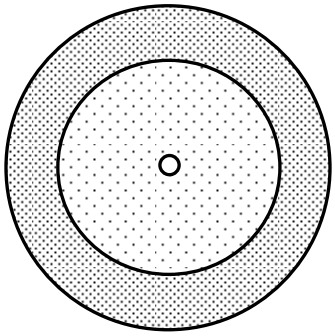

Figure 7. Leaky compartments represented by a two-zone radial model

Table 2. Design Factors and Levels for Leaky-compartment Model

Design Level		Design Factors	
		Pore Volume Multiplier	Transmissibility Between Two Zones
0	Inner Zone Outer Zone	×0.5 ×2	0.1
1	Inner Zone Outer Zone	×2 ×0.5	1

Table 3. Design Configuration for Leaky-compartment Model

Run No.	V	T
1	0	0
2	0	1
3	1	0
4	1	1

The two design levels 0 and 1 are assigned to the factors for each simulation run for a two-level full factorial design according to the table below. There are only 4 simulation runs for this simple design (**Table 3**).

The bottom hole pressures for the buildup from the simulation runs are plotted as log-log plot shown in **Figure 8**:

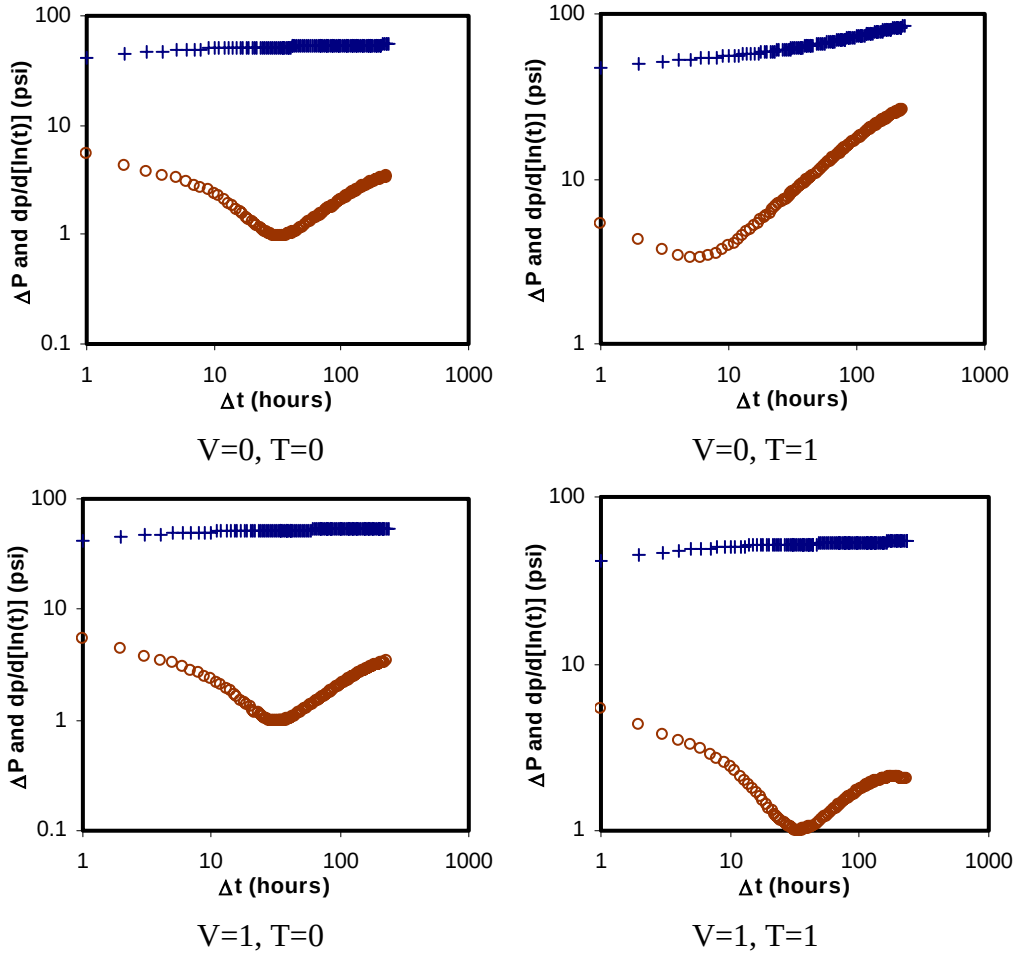

Figure 8. Log-log plots for leaky-compartment model

We can see from the plots in **Figure 8** that there is obvious concave-up shape on the derivative curve, which is caused by the difference between the flow capacity and storage capacity between the two zones. When the reservoir is depleted beyond the partial-communicating barrier, the pressure behavior is like that of double-porosity reservoir, in which the inner zone with higher permeability primarily provides flow capacity and the outer zone with larger pore volume provides storage capacity.

The compartmentalized geometry is often observed in fluvial systems (Junkin and others, 1992). For channelized turbidite reservoirs there may be analogous effects, but for overbank turbidite reservoirs, the lateral leaky-compartment model may be less suitable. However, there is some, currently unpublished, evidence from material balance calculations that the leaky-compartment model may fit pressure declines in turbidite models reasonably well (C. D. White, Personal Communication).

3.3 Rate History Influence

Generally speaking, the influence of flow history on buildup is less than on drawdown. For this reason, buildup analysis is frequently used to determine reservoir parameters than drawdown analysis. Nevertheless, variable flow history distorts buildups especially when the flow rate is decreasing. Streltsova (1988) used the principle of superposition to investigate the influence of different type of variable production rate on the subsequent buildup pressure behavior. She concluded that a flow rate that decreases to a minimum value causes much more distortion in the subsequent buildup than a flow rate that increases to a maximum value prior to shut-in for all cases considered. Three different types of decreasing flow rates including linear, hyperbolic and parabolic are designed for the production before shutin. Their respective function is expressed below and the shape of each rate function is plotted in **Figure 9**.

Linear: $q(t) = q_0(1 - at)$

Hyperbolic: $q(t) = \frac{q_0}{(1 + at)^{1/b}}$

Parabolic: $q(t) = q_0(1 - at^2)$

The influence of each decreasing rate function obtained from reservoir simulation is shown in the log-log plots (**Figure 10**). Compared with the case of constant flow rate, there is upward-rising trend on the derivative curve for the three cases of decreasing flow rate, in which the upward-rising trend is the smallest for the hyperbolic case. The influence of rate history is not very significant. However, if rate variation is neglected, erroneous reservoir model would be identified and incorrect estimates would be obtained for the reservoir parameters in well test analysis. For example, in the case of decreasing rate, we could choose a reservoir model with faults to interpret the upward-rising trend on the derivative curve. Streltsova (1988) suggested that a decreasing rate prior to shut-in should be avoided whenever possible.

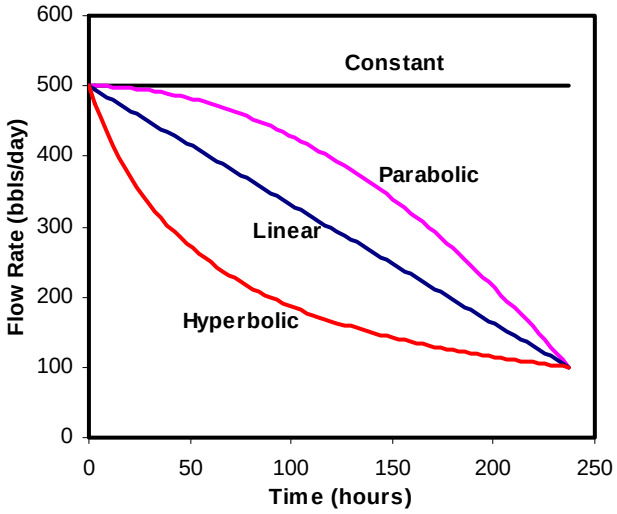

Figure 9. Different types of variable flow rates

3.4 Differential Depletion in Multilayered Models

Channel-levee-lobe turbidite reservoirs should be represented by multilayered models due to their layered character. Multilayered models can be classified by presence of interlayer or formation crossflow. The multilayered reservoir is called a commingled

system if there is no crossflow occurring between the layers, and a crossflow system if there is interlayer crossflow. For a multilayered reservoir, differences in layer properties like permeability, pore volume and skin often lead to unbalanced depletion and poor recovery due to over-depletion for layers with high flow capacity and under-depletion for layers with poor flow capacity. This situation is more serious for commingled reservoir since formation crossflow can mitigate the unbalanced depletion in the crossflow system.

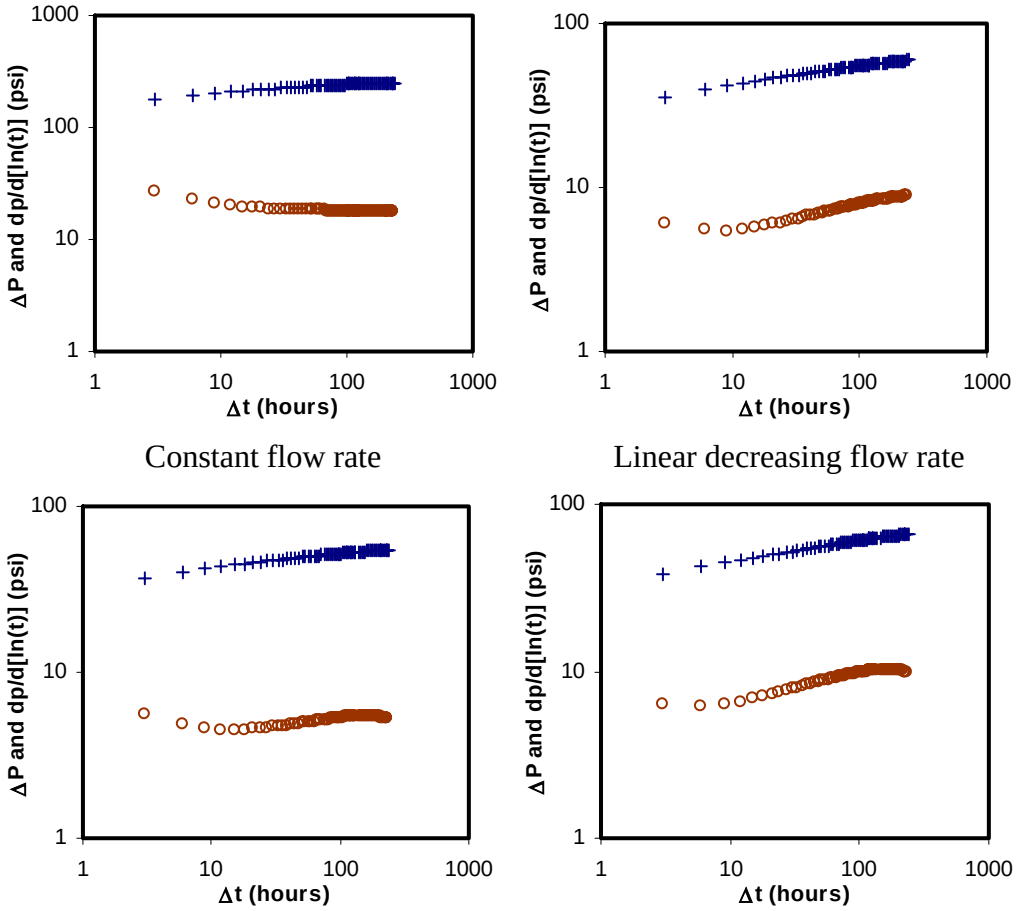

Constant flow rate | Linear decreasing flow rate

Hyperbolic decreasing flow rate | Parabolic decreasing flow rate

Figure 10. Log-log plots for variable decreasing flow rates

Our emphasis is on the commingled system since it is the most probable mechanism causing anomalous pressure behavior. In the next several chapters, we will investigate the pressure behavior of multilayered reservoirs. First we will use a simple two-layer model

to examine the effect of differential depletion on the pressure behavior. Then we will use a three-layer model to represent multilayered system and use experimental design and response surface to relate pressure behavior and reservoir parameters. Also we will investigate how to distinguish the multilayered model and the Leaky-compartment model since the two models have similar pressure response.

3.5 Wellbore Storage Influence

Wellbore storage is known to influence early-time pressure behavior in a homogeneous reservoir, but effects on the pressure behavior in a multilayered reservoir with high contrast in layer properties have not been examined. We use a two-layer model to examine this. The permeability of the layers is fixed, 100 md for layer 1 and 1000 md for layer 2. The wellbore is simulated by assigning a large pore volume value (equal to the wellbore volume) and a large permeability value to the innermost radial grid block. We make a simple 2^2 factorial design according to the design factors and design levels shown in **Table 4**. The factors considered in the design are pore volume and wellbore storage. The two design levels 0 and 1 are assigned to the factors for each simulation run for a two-level full factorial design according to **Table 5**.

Table 4. Design Factors and Levels for Wellbore Storage Effect

Design Level		Design Factors	
		Pore Volume Multiplier	Wellbore Storage
0	Layer 1 Layer 2	×0.5 ×2	No
1	Layer 1 Layer 2	×2 ×0.5	Yes

Table 5. Design Configuration for Wellbore Storage Effect

Run No.	W	V
1	0	0
2	0	1
3	1	0
4	1	1

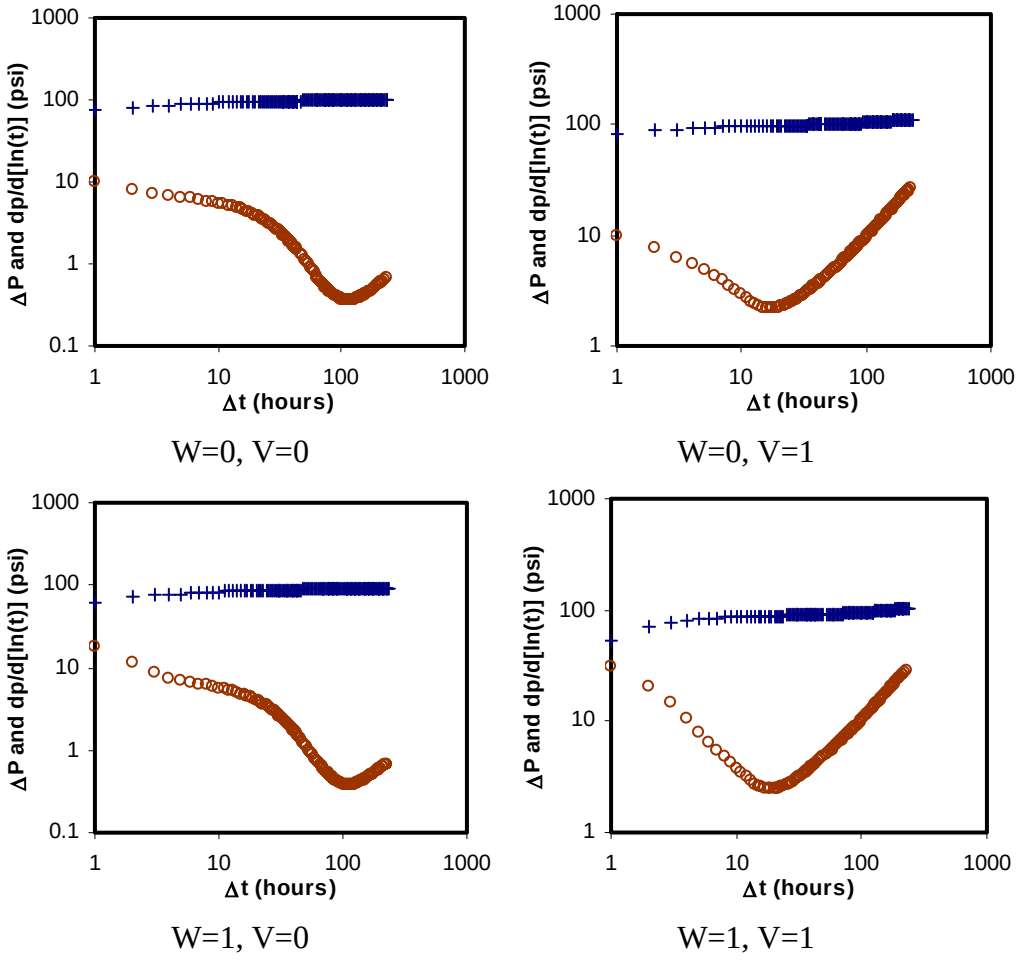

Figure 11. Log-log plots for wellbore storage influence

The influence wellbore storage obtained from reservoir simulation is shown in the log-log plots (**Figure 11**). Comparing the plots for the cases with and without wellbore storage effect, it can be seen that the wellbore storage only has influence on the early-time behavior and has little influence on the late-time behavior even for the reservoir with

high contrast in layer diffusivity. In addition, wellbore storage can often mask the reservoir response and make the pressure derivative useless for interpreting the reservoir behavior. Therefore, in the subsequent analyses, we will not include wellbore storage for the purpose of simplification.

CHAPTER 4. STUDY ON MULTILAYERED SYSTEMS

4.1 Literature Review

The earliest rigorous study for the commingled multilayered reservoir system was made by Lefkovits and others (1961). This study provided an analytic solution to the reservoir model with an arbitrary number of layers with distinct layer properties including thickness, porosity, permeability and skin. A typical theoretical pressure buildup curve was obtained from a two-layer reservoir and the behavior of layer production rate was studied. It is also shown that the time needed to reach pseudosteady state for a multilayered reservoir is much longer than for a single-layer reservoir. There is differential depletion between the layers, the more permeable layer depleting more than the less permeable layer; this takes place before the arrival of pseudosteady state. Skin affects pressure behavior for the entire range of shut-in time for a multilayered reservoir, whereas the effect vanishes after a short period of shut-in time for a single-layer reservoir. In addition, this study illustrated that higher skin in the more permeable layer tends to mitigate the differential depletion. This study further showed that (a) during transient flow the fractional production rate from each layer is approximately equal to the ratio of the flow capacity of each layer to the total reservoir flow capacity during the early transient period; (b) production is proportional to the ratio of pore volume of each layer to the total reservoir pore volume during pseudosteady state. These insights provided a basis for well test analysis in commingled reservoirs.

Cobb and others (1972) investigated various analysis techniques for pressure buildup test with equal thickness and used the solution derived by Lefkovits and gave an approximate relationship between the length of transient state and the permeability ratio

for a two-layer reservoir. They concluded that the length of transient state increases as permeability contrast increases and the late-time buildup pressure increase is the result of differential depletion and is caused by fluid flowing from the lower flow capacity zone (or less depleted zone) to the higher flow capacity zone (or more depleted zone) and this feature can be significant if the permeability contrast and producing time are large. Raghavan and others (1974) extended this study by using unequal thickness for a two-layer reservoir.

Earlougher and others (1974) showed that there is no general description for pressure buildup behavior in layered reservoirs without crossflow, which can be very different from or can be very similar to the behavior of single-layer system. The time required to reach pseudosteady state depends on porosity ratio, permeability ratio, geometry and number of layers.

Tariq and Ramey (1978) included wellbore storage and different layer outer boundary radii into the commingled system and used the Stehfest algorithm for numerical inversion of Laplace transforms. They studied the drawdown behavior and concluded that the length of transient stage of depletion is a function of the permeability ratio, skin effect and the pore volume ratio. The conventional stages of drawdown behavior may be partially or completely obscured by effects of differential depletion in a multilayered reservoir. The presence of a layer of high permeability may act as an extension of the wellbore at early times, further complicating analysis.

For a layered reservoir with interlayer crossflow, Russell and Prats (1962) showed that the pressure and production behavior of a well in such a reservoir is similar to that in a homogeneous reservoir and the total permeability-thickness product is equal to the sum

of permeability-thickness product for each layer. Therefore, the occurrence of interlayer crossflow can be confirmed by the homogeneous-like appearance of the pressure behavior. They also illustrated that interlayer crossflow is beneficial to the production since the tight layers are effectively depleted by the interlayer crossflow to the permeable layers and recovery is increased.

Gao and Deans (1983) used numerical method to verify that wellbore pressure is insensitive to the crossflow for a two-layer system separated by a semi-permeable barrier and the system responds as a single-layer reservoir with a transmissibility equal to the sum of the two layer transmissibilities.

Bourdet (1985) proposed an analytical solution for the double permeability model to describe the pressure response of a two-layer reservoir with crossflow, with the layered system without crossflow as a limiting form of the solution. He illustrated that layered system can produce intermediate pressure behavior between the response of homogeneous system and response of double porosity system. He also concluded that the heterogeneous characteristics of the responses are much more pronounced for large permeability thickness ratios and small storativity ratios.

Ehlig-Economides and Joseph (1987) gave a good review of the history of studies on the behavior of multilayered reservoir systems and proposed analytic solutions to a n-layer reservoir model with or without interlayer crossflow for various outer boundary conditions (infinite acting, no flow and constant pressure) as well as skin and wellbore storage effects, which permits the development of limiting forms for understanding certain characteristic of the multilayered system. They also recommended a data-

acquisition scheme and corresponding interpretation procedure for determination of individual layer properties in a multilayered reservoir.

Streltsova (1988) had excellent description on fluid flow in a stratified reservoir. For a reservoir with interlayer crossflow, the layer diffusivity contrast determines both the flow direction and the amount of interlayer crossflow. The storage contrast between layers determines the duration of the transitional flow period and the transmissibility contrast is responsible for the relative contribution of each layer to the total production as long as the skin in each layer is comparable. For a commingled reservoir, crossflow can take place only through the wellbore. The pressure pattern for this case differs significantly from that for interlayer crossflow. During production, when the well flowing pressure is higher than that of the layer with lower pressure, only a portion of the total flow from the layer with higher pressure is produced at the surface. The remainder goes into the layer with lower pressure through crossflow in the wellbore. When the well flowing pressure is lower than that of the lower pressure layer, both layers contribute to the surface production. During ensuing shutin, crossflow develops in the wellbore from the less depleted layers into the more depleted layer, which causes the buildup curve to have a different shape from the drawdown curve. If all layers have limited extent, the buildup curve finally stabilizes at late times at a static pressure dependent on the total system volume and total fluid withdrawal.

4.2 Two-layer Model

A simple two-layer model was created to examine the factors like permeability, skin, pore volume, crossflow and compaction. The model is radial with homogeneous and isotropic properties horizontally (**Figure 12**). Permeability in vertical direction is

changed by adjusting the ratio of vertical to horizontal permeability to allow different degrees of crossflow. Permeability for the two layers is fixed for the two layers, 100 md for layer 1 and 1000 md for layer 2. The dimension of the grid is 68×1×2 with a total area of 80 acres or a radius of 1008 ft. All models contain slightly-compressible undersaturated oil. The well is open for flow for 10 days and shut in for pressure buildup for 10 days. Bottom hole pressure is recorded every three hours.

4.2.1 Two-layer Model for Compaction Effect

The concave-up shape on the Horner plot and rapid upward-rising on the derivative curve of the log-log plot is most likely caused by differential depletion due to contrast of permeability, skin and pore volume between the layers. However, compaction may also contribute to this phenomenon. Typical deepwater reservoirs in Gulf of Mexico are unconsolidated to slightly consolidated turbidite sands. Such sands are prone for considerable compaction for large pressure drawdowns due to high flow rate during the production of the reservoir (Ostermeier, 2001). Significant permeability reduction can be expected due to compaction as the reservoir pressure depletes. Permeability reduction appeared more severe near the wellbore (Petro and others, 1997). On a relative basis, compaction reduces permeability four to five times more than it reduces porosity (Ostermeier, 2001).

To assess the effects of differential depletion and compaction, a two-level full factorial experimental design is conducted on a simple two-layer radial model (**Figure 12**) with no crossflow across the two layers. Permeability is fixed for the two layers, 100 md for layer 1 and 1000 md for layer 2. The factors considered in the design are skin factor, pore volume and compaction. The compaction effect is included in the model by

modifying the pore volume and transmissibility of the reservoir by the multipliers shown in **Table 6**. The compaction effect is set to irreversible, i.e., the pore space does not re-inflate when the pressure increases, considering the unconsolidated nature of the reservoir rock in the Gulf of Mexico. The factor values are assigned to the two layers according to **Table 7**.

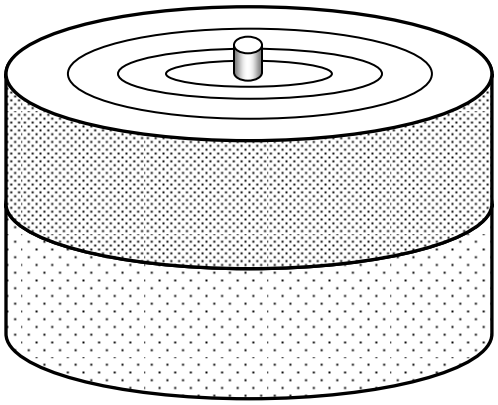

Figure 12. Schematic graph of 2-layer radial model

Table 6. Compaction Effect Table

Pressure psi	Pore Volume Multiplier	Transmissibility Multiplier
500	0.968	0.830
1000	0.970	0.850
2000	0.980	0.900
3000	1.000	1.000

The two design levels 0 and 1 are assigned to the factors for each simulation run for a two-level full factorial design according to **Table 8**.

Table 7. Design Factors and Levels for Compaction Model

Design Level		Design Factors		
		Skin	Pore Volume Multiplier	Compaction
0	Layer 1	5	×0.5	No
	Layer 2	50	×2	
1	Layer 1	50	×2	Yes
	Layer 2	5	×0.5	

Table 8. Design Configuration for Compaction Model

Run No.	S	V	C
1	0	0	0
2	0	0	1
3	0	1	0
4	0	1	1
5	1	0	0
6	1	0	1
7	1	1	0
8	1	1	1

In the above table, S stands for skin, V for pore volume and C for compaction. Eight simulation runs are conducted on the 2-layer radial model. The model has the grid dimension 71×1×2. The bottom hole pressures for the buildup from the simulation runs are plotted as log-log plot. The plot for each simulation run is shown in **Figure 13**.

From the plots, we can see that the rapid upward-rising on the derivative curve occurs when permeability and pore volume are in contrast in the two layers, i.e., higher permeability corresponds to smaller pore volume and vice versa, and skin is in contrast to permeability, i.e., higher permeability corresponds to lower skin and vice versa. In the above design, $k_1/k_2 = 0.1$, $V_1/V_2 = 4$ and higher skin is in the less permeable layer 1.

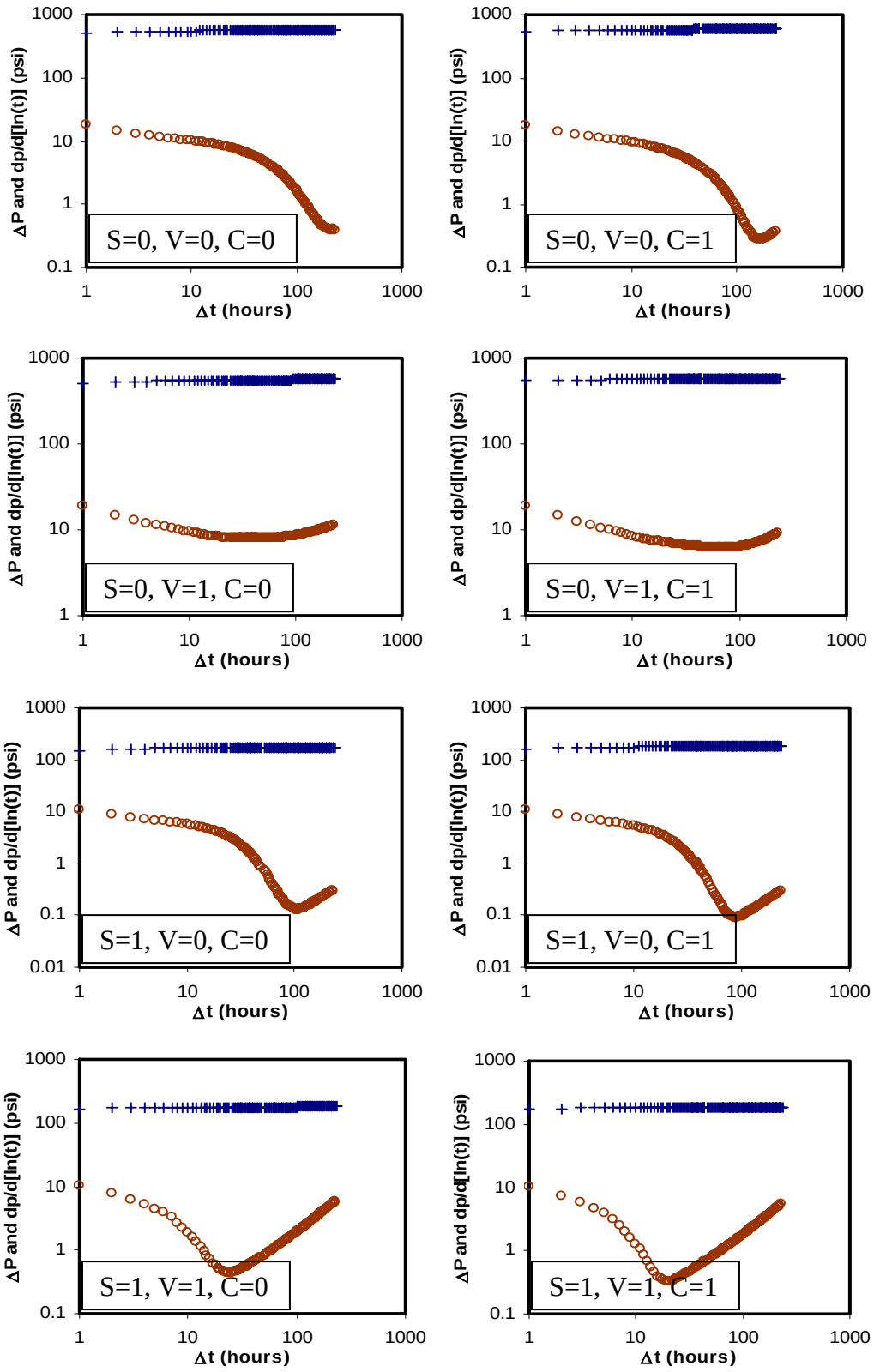

Figure 13. Log-log plots for the design for skin, pore volume and compaction

Compaction has very small influence on the pressure behavior. A Horner plot corresponding to the case of permeability in contrast to pore volume and skin is shown below (**Figure 14**). We can see that there is obvious concave-up trend on the Horner plot, which is rather similar to the phenomenon observed in the Ram-Powell oilfield. The layers are depleted differently during production due to permeability contrast, which would result in big difference in the layer average pressure if the production is long enough. After shut-in, the more depleted layer will get flow from the less depleted layer besides its own pressure equalization. This will cause the acceleration of the pressure buildup, and this process will last for a long time until the pressures in both layers are balanced. This is the reason for the appearance of the concave-up shape during buildup.

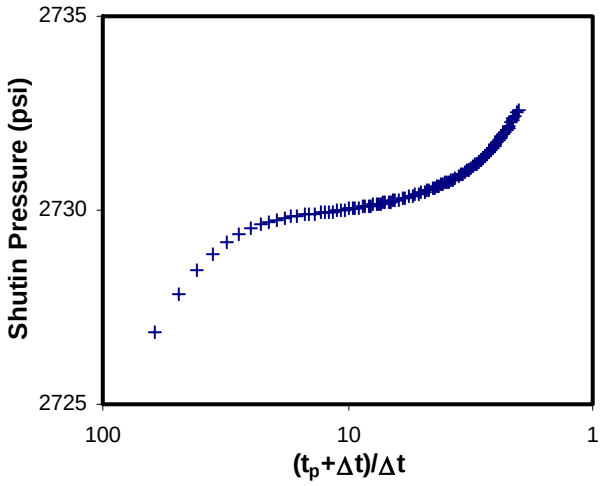

Figure 14. Horner plot for the case of permeability in contrast to pore volume

4.2.2 Two-layer Model for Crossflow Effect

Crossflow occurring between communicating layers is called interlayer or formation crossflow, which is not included in the above design. However, formation

crossflow may have significant effect on the pressure behavior. To examine the effect of formation crossflow, a new 2-level design including only skin, pore volume and crossflow is conducted on the same 2-layer radial model. The factor values are assigned to the two layers according to **Table 9**.

Table 9. Design Factors and Levels for Crossflow Model

Design Level		Design Factors		
		Skin	Pore Volume Multiplier	Crossflow
0	Layer 1	5	×0.5	No
	Layer 2	50	×2	
1	Layer 1	50	×2	Yes
	Layer 2	5	×0.5	

The two design levels 0 and 1 assigned to the factors for each simulation run for a two-level full factorial design according **Table 10**.

Table 10. Design Configuration for Crossflow Model

Run No.	S	V	X
1	0	0	0
2	0	0	1
3	0	1	0
4	0	1	1
5	1	0	0
6	1	0	1
7	1	1	0
8	1	1	1

In **Table 10**, S stands for skin, V for pore volume and X for crossflow. The formation crossflow is realized by setting vertical permeability equal to 0.1 of the horizontal permeability.

Eight simulation runs are conducted on the 2-layer radial model. The bottom hole pressures for the buildup from the simulation runs are plotted as log-log plot. The plot for each simulation run is shown in **Figure 15**.

It can be seen that no matter how different the properties between the two layers and, the pressure behaviors for all cases with crossflow between the layers are similar. The upward-drift behavior on the derivative curve disappears. The reason is that the crossflow due to contrast of flow capacity and storage capacity between the layers occurs through the formation instead of through the wellbore and the differential depletion does not exist. The pressure behavior of 2-layer reservoir model with formation crossflow is just like the behavior of single-layer reservoir.

To examine what happens in the wellbore with and without formation crossflow, the flow rates for the two layers are plotted corresponding to the above 8 simulation runs in **Figure 16**. We can see that the layer flux distribution for the cases with crossflow is much simpler than that for the cases without crossflow. For all the cases with formation crossflow, the layer flow rates remain constant during production proportional to their respective flow capacity and become zero after shut-in. There is no differential depletion because the two layers can stabilize each other in the reservoir through crossflow during production. For the four cases without crossflow, the degree of differential depletion varies. The most serious one occurs in the case with the most contrast between flow capacity and storage capacity. In this case, oil flows from less permeable layer to more

permeable layer through the wellbore after shut-in due to over-depletion in the more permeable layer during production. The flow rate is rather stable due to pressure difference between the layers.

4.2.3 Asymmetry Between Drawdown and Buildup Under Differential Depletion

The asymmetry of pressure behavior between drawdown and buildup is obviously caused by the wellbore crossflow. During production, both the two layers flow to the wellbore; flow is parallel in the two layers. Moreover, the individual layer rates vary for the commingled case, but are constant for the crossflow case. In contrast, during buildup flow is directed from the layer with higher pressure to the layer with lower pressure through the wellbore and the layer resistances are arranged serially. This is the difference between pressure drawdown and buildup (**Figure 17**). Corresponding to the case in which most serious differential depletion occurred, the log-log plots for drawdown and buildup have distinct features (**Figure 18**). The early-time behavior for drawdown is obvious in transient or infinite acting state and the late-time behavior is boundary effect. However, there is no clear radial flow regime exhibited on the early-time derivative curve for buildup. The pressure behavior for buildup is more like that in double-porosity media.

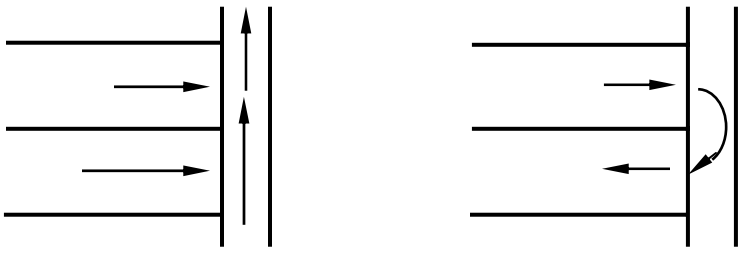

Figure 15. Different flow profile for drawdown and buildup

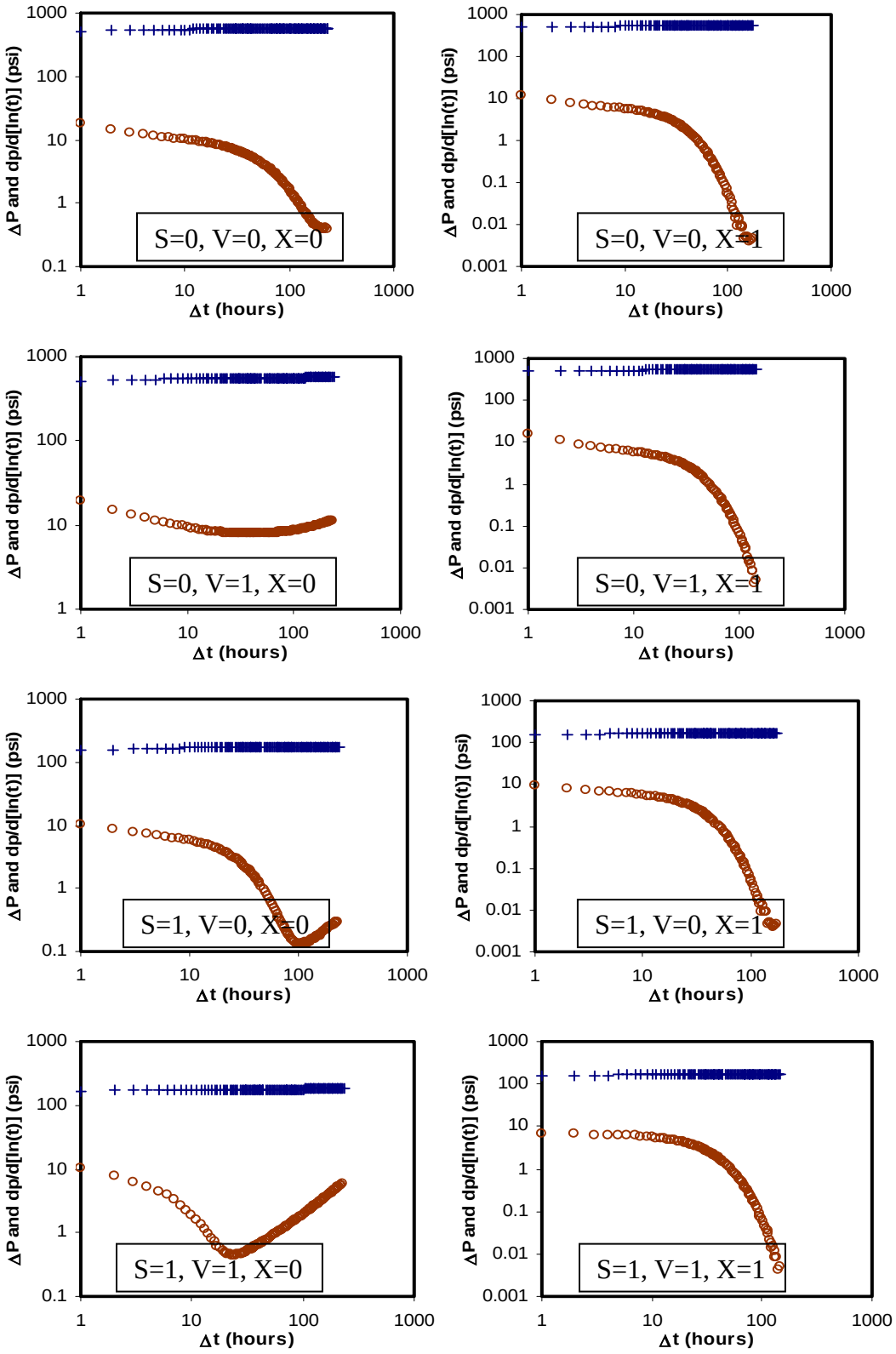

Figure 16. Log-log plots for the design for skin, pore volume and crossflow

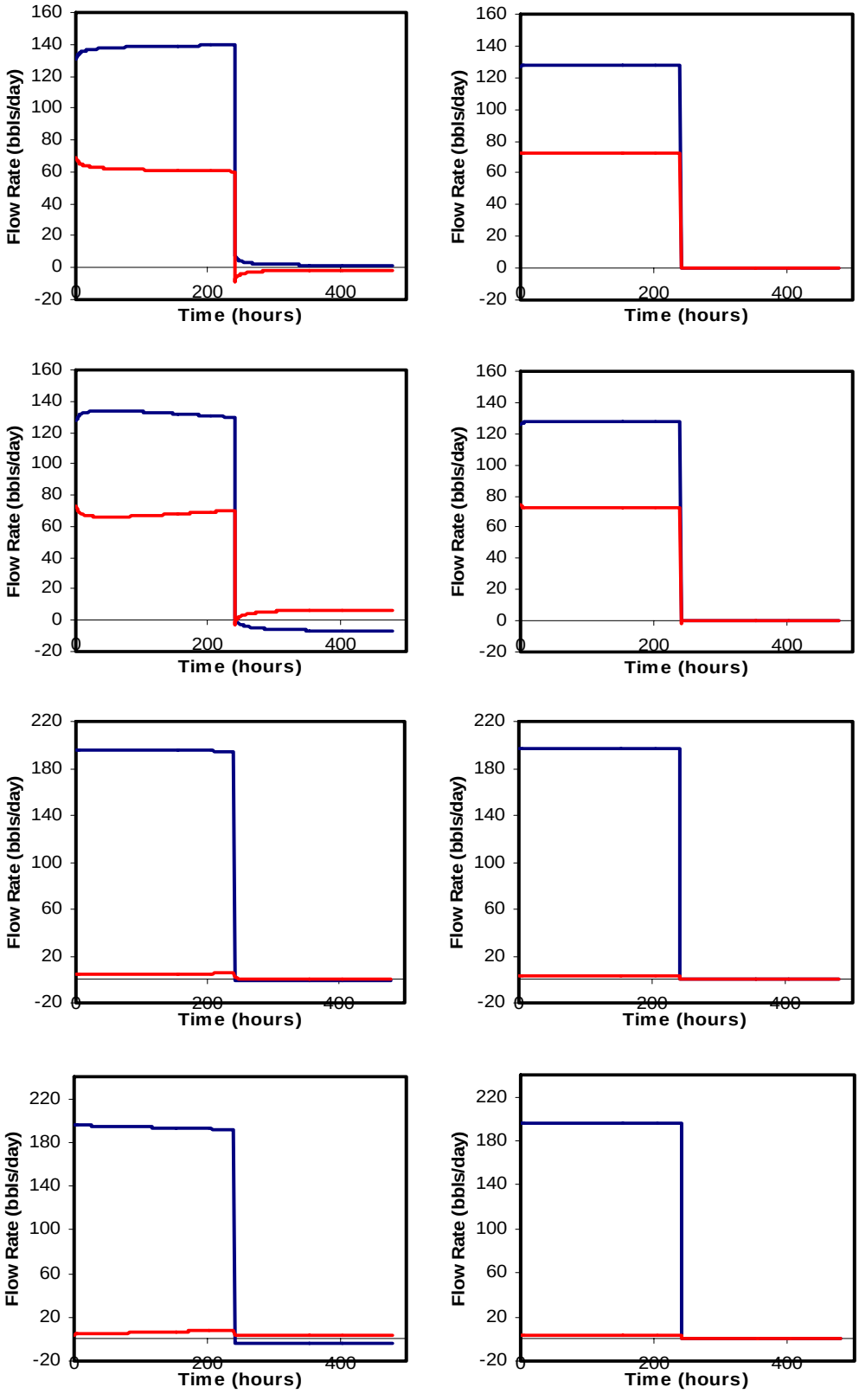

Figure 17. Layer flow rates for the design for skin, pore volume and crossflow

During production, the contrast between flow capacity and storage capacity causes pressure imbalance between the two layers; the imbalance increases with increasing permeability contrast. However, during pressure buildup, the layer with low flow capacity will become an obstruction to the wellbore crossflow, which would reduce the degree of differential depletion. We verify this by choosing the case with the most significant differential depletion (S=1, V=1, X=0) and changing the permeability of less permeable layer and see what would happen for the pressure derivative curve and layer flow rates.

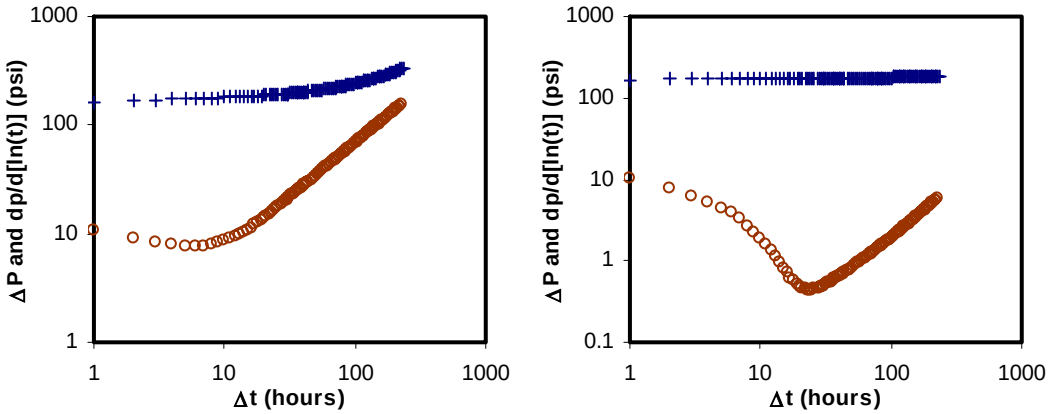

Figure 18. Log-log plots for drawdown and buildup

The increase of the permeability for the less permeable layer enhances the upward-rising trend on the derivative curve by increasing the wellbore crossflow. This indicates that differential depletion may occur through pore volume contrast with skin factor regardless of flow capacity difference between the layers. Significant pressure difference can be established between layers either through pore volume contrast with skin factor or permeability. Differences in *kh* are not the sole cause for differential depletion and wellbore crossflow.

4.3 Multilayered Model

The results from the two-level full factorial design for the two-layer model are significant enough to warrant a more complicated multilayered model (which is more similar to the real reservoir) and more factors and levels should be considered. Factors that have influence on pressure behavior as discussed in the section of two-layer model are included in the model. Factors of potential interest were varied using experimental design, and their effects were assessed using response surface method. These methods are discussed in texts (Myers and Montgomery, 1995) and in the reservoir engineering literature (White and Royer, 2003).

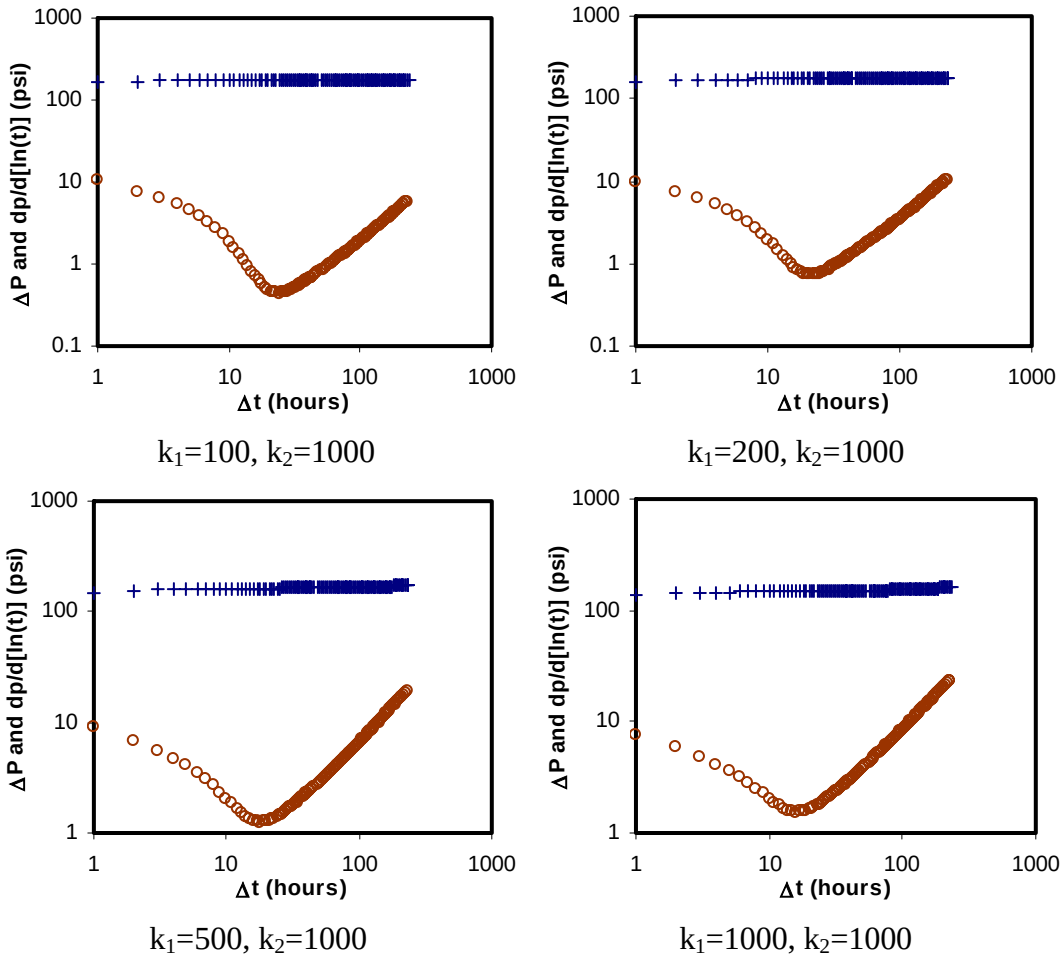

Figure 19. Log-log plots for varying first-layer permeability

All responses are based on characteristics of the derivative curve from well test interpretation. This sensitivity study investigates whether complex derivative behavior can be caused by variations in layer permeability, skin, and non-uniform flux distributions at the well. A three-layer model is used to represent the multilayered reservoir since we can group the thin turbidite reservoir layers into three layers with low, medium and high capacity respectively according to their layer properties such as permeability. Moreover, a three-layer model is easier to control for the purpose of experimental design. We will look into the pressure behavior of commingled system and crossflow system respectively.

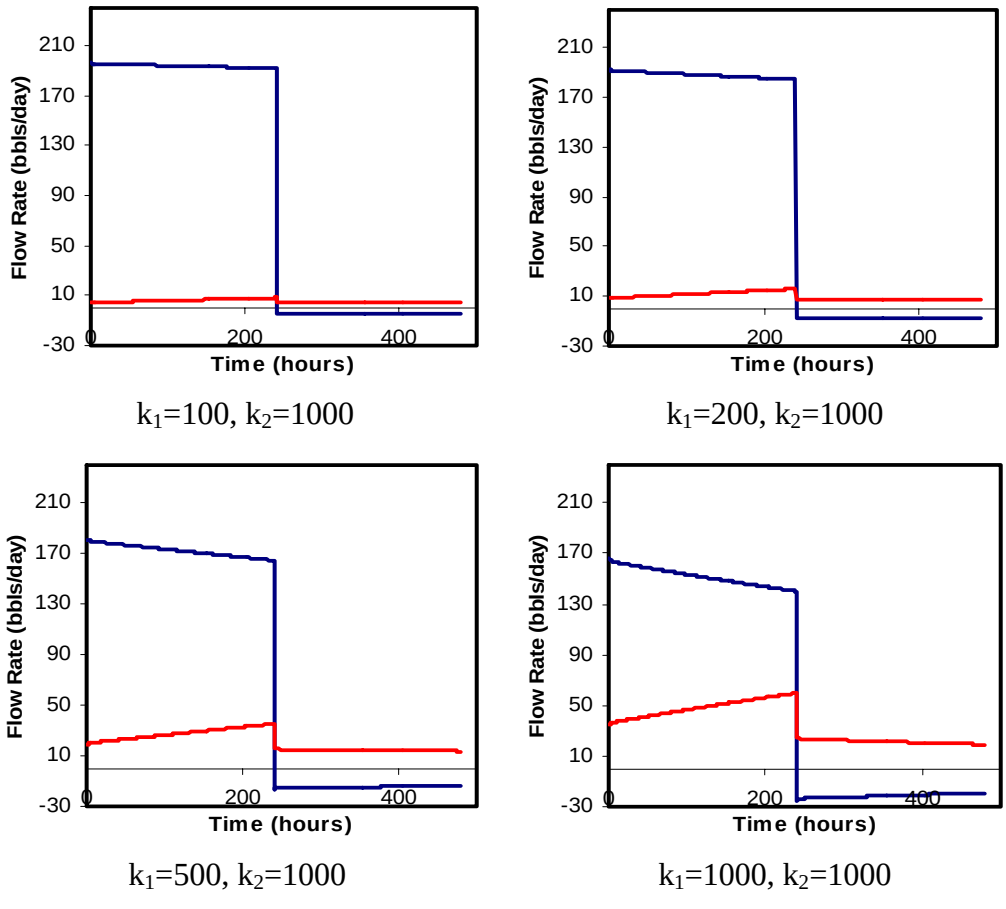

k_1=100, k_2=1000 k_1=200, k_2=1000

k_1=500, k_2=1000 k_1=1000, k_2=1000

Figure 20. Layer flow rates for varying first-layer permeability

4.3.1 Simulation Models

Like the two-layer model, a radial geometry was used for the models with one well in the center. The grid dimensions are 71×1×3 depending on the area of the reservoir (71 in r, 1 in θ, 16 in z direction) (**Figure 21**). The grid size in r direction is chosen so that finer grid size would give almost no change to the pressure response. The models are orthotropic (same permeability in θ and r directions, different permeability in z direction). All models contain slightly-compressible undersaturated oil; no multiphase flow occurs. The well is open for flow for 10 days and shut in for pressure buildup for another 10 days. Bottom hole pressure is recorded every three hours.

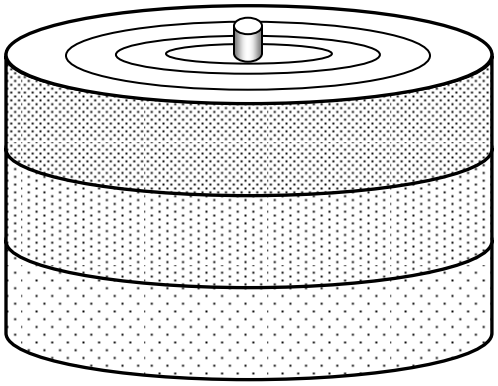

Figure 21. Schematic graph of 3-layer radial model

4.3.2 Factors Considered

We fix the properties of the second layer and vary the properties of the first layer and the third layer. This is realized by using ratios of permeability, pore volume and skin to the second layer as the design factors. The crossflow between layers is accounted for by the ratio of vertical to the horizontal permeability. For commingled system, the factor

k_z/k_h is not needed, but it is needed for crossflow system. In order to use the same 7-factor experimental design pattern for both systems, we can set k_z/k_h to zero for all three levels for the commingled system. The factors considered and their design ranges are given in **Table 11**.

Table 11. Design Factors and Value Ranges Used for 3-Layer Model

Design Level	k_1/k_2	k_3/k_2	V_1/V_2	V_3/V_2	s_1/s_2	s_3/s_2	k_z/k_h	
							Commingled	Crossflow
-1	0.1	0.1	0.2	0.2	0.2	0.2	0	0.001
0	1	1	1	1	1	1	0	0.01
1	10	10	5	5	5	5	0	0.1

4.3.3 Experimental Design

Combinations of factors were chosen to span the factor space. A Box-Behnken design (similar to that used in the Glider study; White and Royer, 2003) was used because (a) it is efficient and (b) it can model quadratic terms (making the model more accurate). A sketch of a Box-Behnken design in three dimensions illustrates the principle that combinations on hypercube edges and at the hypercube centerpoint are used and a large number of design points (or simulation runs) are saved (**Figure 22**).

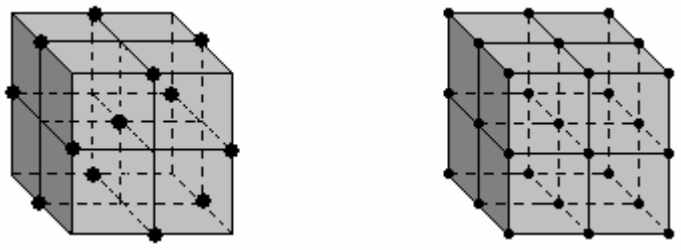

Figure 22. Box-Behnken design and 3-level full factorial design

For the seven-dimensional study undertaken here, 57 simulations are needed. These runs are specified in a design file (**Table 12**). The notation ±1 indicates both levels are to be run in all possible combinations with other ±1 values on the row. Because there are three such values per row, the first seven rows represent 8 simulations each (total of 56) and the last row specifies the centerpoint (1 more run; total of 57 runs). We can see that for each row, the number of 0s and ±1s is the same, and for each column, the number of 0s and 1s is the same as well. The Box-Behnken design is a very balanced design.

Table 12. Box-Behnken Design for 7 Factors

k_1/k_2	k_3/k_2	V_1/V_2	V_3/V_2	s_1/s_2	s_3/s_2	k_z/k_h
0	0	0	±1	±1	±1	0
±1	0	0	0	0	±1	±1
0	±1	0	0	±1	0	±1
±1	±1	0	±1	0	0	0
0	0	±1	±1	0	0	±1
±1	0	±1	0	±1	0	0
0	±1	±1	0	0	±1	0
0	0	0	0	0	0	0

4.3.4 Response Models

The purpose of building the three-layer model is to examine the sensitivity of the pressure derivative curve of the log-log plot to different layer properties and wellbore parameters (or their interactions) and screen out those insignificant factors. We can then use a smaller number of factors and see how they influence the pressure derivative curve by varying their values. We choose the derivative curve because this curve is very sensitive to changes in different influencing factors and is widely used for diagnosis of flow regimes. Indeed, the anomalous derivative is the diagnostic feature for the behavior being investigated here. The derivatives are calculated numerically from the simulated pressure behavior using a non-centered finite-difference expression (Horne, 1995):

$$\frac{dP}{d\ln t}(t_i) = \frac{\ln(t_i / t_{i-k})\Delta P_{i+j}}{\ln(t_{i+j} / t_i)\ln(t_{i+j} / t_{i-k})} + \frac{\ln(t_{i+j} t_{i-k} / t_i^2)\Delta P_i}{\ln(t_{i+j} / t_i)\ln(t_i / t_{i-k})} - \frac{\ln(t_{i+j} / t_i)\Delta P_{i-k}}{\ln(t_i / t_{i-k})\ln(t_{i+j} / t_{i-k})} \quad \ldots(5)$$

The forward and backward differencing increments (j and k) are selected to filter noise in the numerical solution ($\log\left(\frac{t_{i+j}}{t_{i-k}}\right)$ is usually taken to be at least 0.2). Wellbore storage has not been included in these simulations.

We examine the set of 57 simulations to determine which of the varying factors are influencing the derivative for pressure buildup. The sensitivity of derivative curve shape to the varying factors was examined by fitting piecewise polynomials (in time) to the pressure derivative curve of each of the 57 simulated cases. The derivative data are divided into two sections (**Figure 23**). However, we do not know the joint point connecting the two sections *a priori*, so we cannot fit the two sections independently. In

piecewise regression, the appropriate joint point is sought and the two sections are fitted simultaneously. The two fitted polynomials interact with each other during the process of regression since they share the same piecewise regression model. We fit the logarithm of pressure derivative versus the logarithm of time instead of pressure derivative versus time since what we look into is the shape of the pressure derivative curve on the log-log plot. The piecewise regression model is:

$$\hat{y} = \alpha_0 + \alpha_1 x + \alpha_2 x^2 + \alpha_3 (x - x_j)c + \alpha_4 (x - x_j)^2 c + \alpha_5 (x - x_j)^3 c \quad \text{.....(6)}$$

where $\hat{y}$ is the logarithm of pressure derivative, x is the logarithm of the equivalent time t_e, which is defined in the equation below:

$$t_e = \frac{t_p \Delta t}{t_p + \Delta t} \quad \text{.....(7)}$$

c is a constant. When $x \le x_j$, $c = 0$, the fitted curve is a second-order polynomial; When $x > x_j$, $c = 1$, the fitted curve is a third-order polynomial. $x_j = \log(t_j)$ is the point at which the curve shape changes to some extent and the two fitted polynomials coincide. The joint point x_j is determined automatically by a SAS nonlinear regression procedure (SAS/STAT User's Guide), at which both fitted polynomials have reached best fit. The coefficients α_k (k = 0, 1, …, 5) are the coefficients to be fitted. The nonlinear procedure requires that initial values for the coefficients and the joint point. We choose $t_j = 30$ or $x_j = 1.477$ as the initial value for the joint point because most derivative curves seem to have a inflection point near this time value according to our observation, and fit a second-

order polynomial and a third-order polynomial to the two sections divided by the fixed joint point respectively. The initial value for the piecewise regression model is estimated from these coefficients. From these initial values, the nonlinear procedure calculates the coefficients α_k and the joint point x_j iteratively until convergence.

After we have the α_k and the t_j value, we can easily obtain the two fitted polynomials:

$$\hat{y}_1 = \alpha_0 + \alpha_1 x + \alpha_2 x^2, x \le x_j \quad \text{.....(8)}$$

for the first section of derivative data and

$$\hat{y}_2 = (\alpha_0 - \alpha_3 x_j + \alpha_4 x_j^2) + (\alpha_1 + \alpha_3 - 2\alpha_4 x_j)x + (\alpha_2 + \alpha_4)x^2 + \alpha_5 x^3, x > x_j \quad \text{.....(9)}$$

for the second section of derivative data. Equations (8) and (9) can be derived from the piecewise model Equation (6). The first polynomial and the second polynomial are a simple representation of early- to middle-time behavior and middle- to late-time behavior, respectively (**Figures 23**). The fitted derivative curve characteristics are entirely controlled and described by the piecewise polynomial coefficients (**Table 13**). The first section is only dependent on the first three coefficients α_0, α_1 and α_2. However, although the second section is mainly controlled by the last four coefficient α_3, α_4, α_5 and x_j, it is influenced by the first three coefficient α_0, α_1 and α_2 (Eqn. 9). α_2 and α_5 essentially affect tail part of the two sections. This can be seen more visually from **Table 14**, in which the graphs indicate how the pressure derivative curve in log-log plot change corresponding to the increase or decrease of the α values.

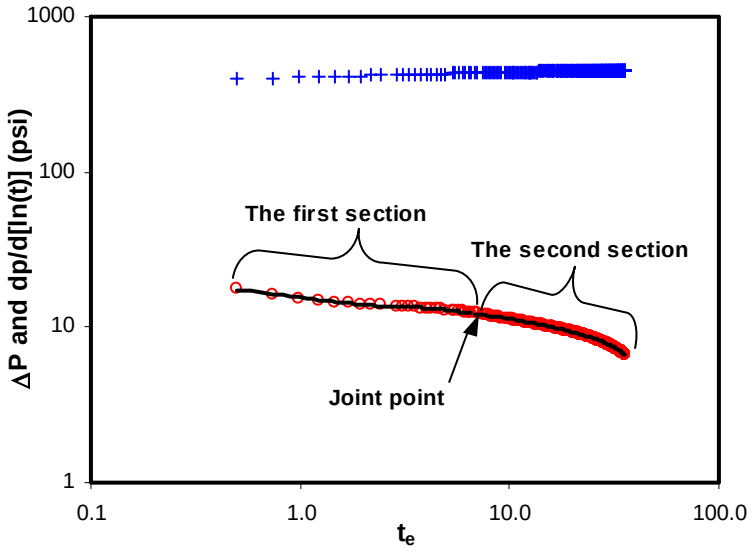

Figure 23. Piecewise regression for the derivative data

The joint point is searched and the two sections are regressed simultaneously by the piecewise nonlinear regression procedure until both sections reach best fit. The first section is fitted by a second-order polynomial and the second section is fitted by a third-order polynomial.

Table 13. Relationship between Coefficients and Derivative Curve Shape

Piecewise Polynomial Coefficients	Corresponding Derivative Curve Shape Characteristics
α_0	Intercept or level of the whole curve; related to permeability
α_1	Slope of the whole curve; reflects inner boundary conditions like skin
α_2	Curvature of the whole curve; reflects the degree of upward or downward drift of the whole curve at transition point
α_3	Slope of the second section; reflects upward or downward drift at late time depending on outer boundary condition
α_4	Curvature of the second section; reflects the degree of upward or downward drift at late time depending on outer boundary conditions
α_5	Near-end curvature of the second section; reflects the degree of upward or downward drift at very late time depending on outer boundary conditions
x_j	Inflection point after radial flow; reflects the occurring time of the flow regime transition point

For the commingled system, the derivative curve can display either upward drift (one example shown in **Figures 24**) or downward drift trend (one example shown in **Figures 25**) depending on the properties of the layers. Two examples of the regression results are shown as black curves in **Figures 24** and **25**, with the equations for two sections given as well, which are actually calculated from the fitted piecewise non-linear equation. These curves fit the derivative data almost perfectly. The motivation for examining the polynomial coefficients is that factors that change these coefficients are the factors that control derivative shape. We are not seeking to build a model for derivative shape, but rather are working to identify the influential factors.

The responses to be modeled are the coefficients of the piecewise polynomials for all 57 points. All the six coefficients and the joint point in the piecewise regression model were independently fitted to distinct models with an intercept, linear terms, two-term interactions, and quadratic terms in all factors; each model could contain up to 36 terms:

$$\hat{\alpha}_k = \beta_{0k} + \sum_{i=1}^{7} \beta_{ik} x_i + \sum_{i=1}^{7} \sum_{j=i+1}^{7} \beta_{ijk} x_i x_j + \sum_{i=1}^{7} \beta_{iik} x_i^2 \quad \text{.....(10)}$$

where $\hat{\alpha}_k$ (k = 0, 1, …, 5) are the estimated coefficients of the fitted piecewise polynomials, which are used as the response variables here. x_i indicates the i^{th} factor, i.e., the permeability ratio, skin ratio, pore volume ratio and the vertical to horizontal permeability ratio of the three formation layers. β's are the coefficients of the terms in the response model. This quadratic form of model is common in analysis of Box-Behnken designs, which can take account of nonlinear effects and interaction effects of the factors.

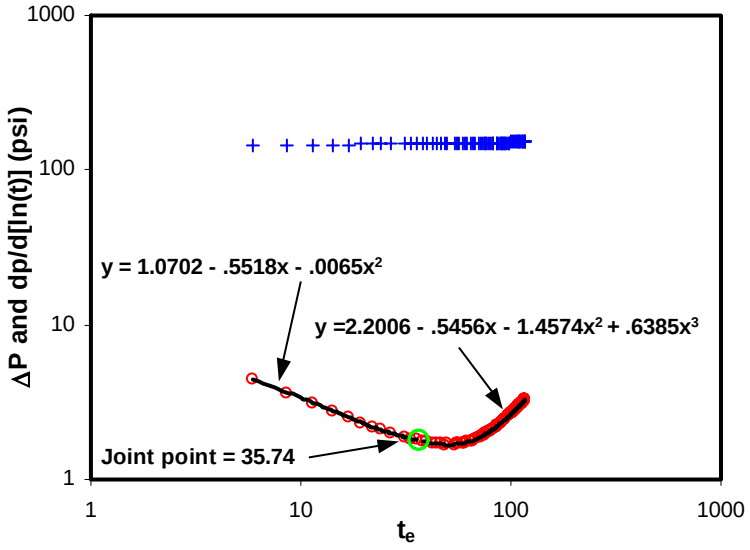

Figure 24. Example 1 for commingled system with piecewise regression

This example corresponds to the factor combination [+1, +1, 0, -1, 0, 0, 0] (**Table 12**), corresponding design values are [10, 10, 1, 0.2, 1, 1, 0] (**Table 11**).

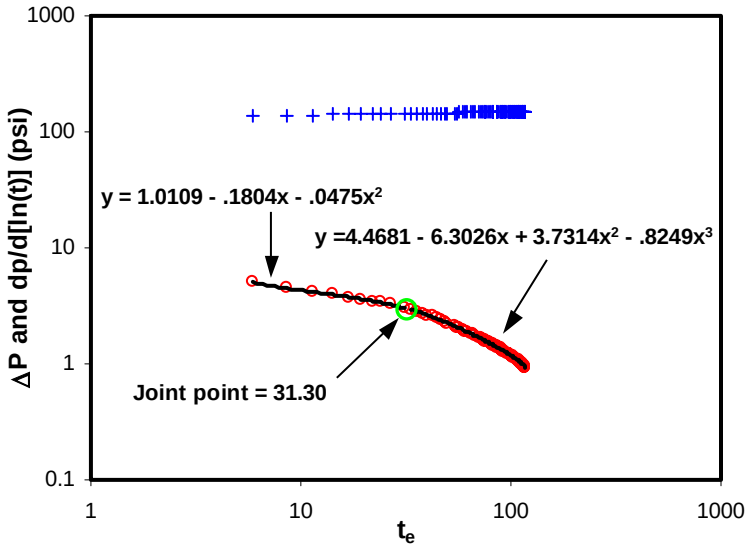

Figure 25. Example 2 for commingled system with piecewise regression

This example corresponds to the factor combination [[+1, +1, 0, +1, 0, 0, 0] (**Table 12**), corresponding design values are [10, 10, 1, 5, 1, 1, 0] (**Table 11**).

Table 14. Pressure Derivative Curve Change with α value

Piecewise Polynomial Coefficients	Corresponding Derivative Curve Shape Change	
	Increase of α value ⬆	Decrease of α value ⬇
Original Curve	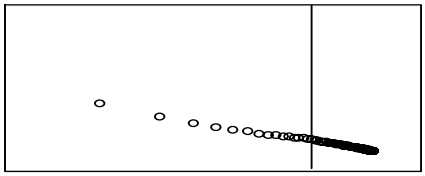	
α_0	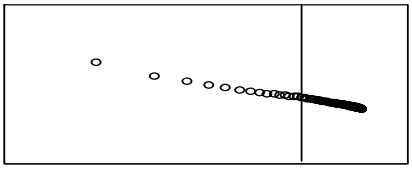	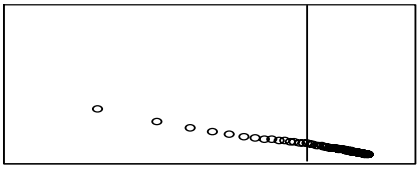
α_1	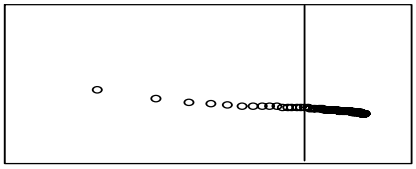	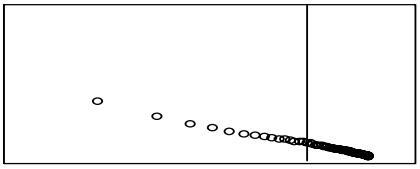
α_2	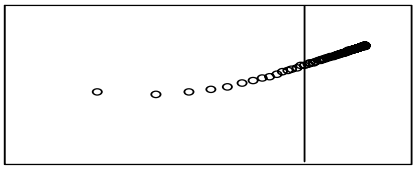	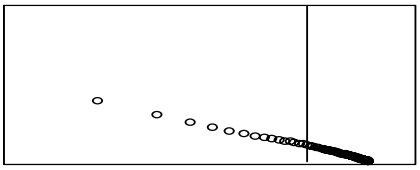
α_3	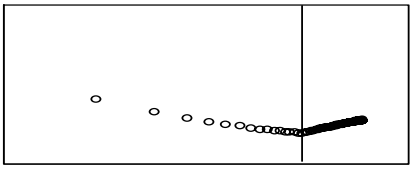	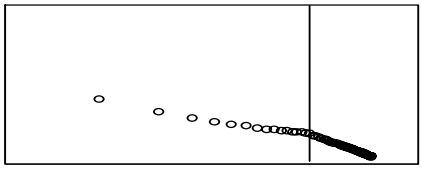
α_4	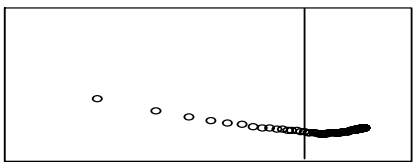	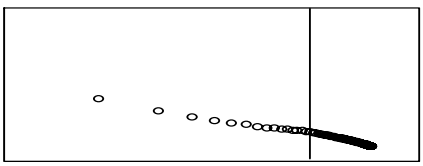
α_5	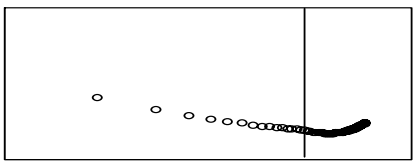	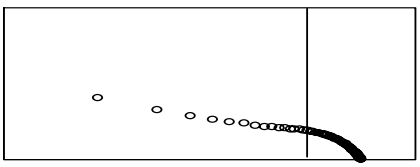
x_j	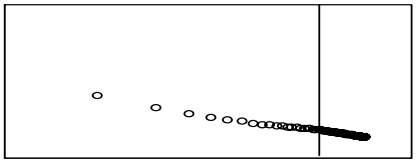	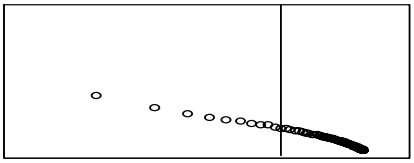

4.3.5 Significant Factors for Commingled System

After fitting the response model (Eqn. 10) for the commingled system, no model contains more than 7 terms of the 36 possible terms, and only 12 terms are significant for all 7 coefficients combined (**Table 15**). This anticipated simplification was the motivation of the response modeling.

We choose 0.05 as the significance level, which means the probability that a significant factor is insignificant is below 0.05, or we have at lease 95% confidence that a factor is significant or not. The permeability ratio k_1/k_2 and k_3/k_2 affects the most coefficients either directly or via interactions with other variables, which indicates that permeability influence the whole pressure behavior. The skin ratios s_1/s_2 and s_3/s_2 combined with pore volume and permeability affect all of the coefficients, which verified that skin factor influences not only the early time behavior, but also the middle and late time behavior for the commingled system. This indicates there must be flow from one layer to another through the wellbore during shutin. The pore volume ratios V_1/V_2 and V_3/V_2 and their interaction with permeability affect only α_3, which determine the middle time or transitional behavior. The transition point x_j is controlled by almost all the factors. The late time behavior is mainly determined by permeability and skin contrast. The magnitude of influence of the factors or factor interactions on the value of α's can be seen more directly by the bar graph shown in **Table 16**. The bigger the absolute value of the coefficient, the bigger influence on the derivative curve shape it has. There is no surprise in the results, however, we can see the effectiveness of the experimental design to perform the sensitivity analysis and screen the potential influential factors.

Table 15. Significant Terms for Commingled System

Factor or interaction	α_0	α_1	α_2	α_3	α_4	α_5	x_j
k_1/k_2	-0.4452	0.1939	-0.1183		-1.3866	2.4319	1.9082
k_3/k_2	-0.4353	0.1819	-0.1224			1.9352	1.7063
$k_1/k_2*k_1/k_2$	-0.1843						2.6708
$k_3/k_2*k_1/k_2$	0.3114	-0.3046	0.1870	-0.2097			-3.0176
$k_3/k_2*k_3/k_2$	-0.2856		-0.1297				2.9625
V_1/V_2				-0.1333			
V_3/V_2				-0.1150			
$V_3/V_2*V_1/V_2$							2.8272
$V_1/V_2*k_1/k_2$				-0.2833			
$V_3/V_2*k_3/k_2$				-0.2486			
$s_1/s_2*V_1/V_2$				0.1870			
$s_3/s_2*k_3/k_2$	0.1864	-0.2919	0.1457		2.2551	-4.4532	-3.5487
All other terms are insignificant							

Table 16. Bar Graph for Significant Terms for Commingled System

Factor or interaction	α_0	α_1	α_2	α_3	α_4	α_5	x_j
k_1/k_2	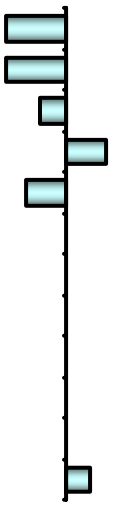						
k_3/k_2							
$k_1/k_2*k_1/k_2$							
$k_3/k_2*k_1/k_2$							
$k_3/k_2*k_3/k_2$							
V_1/V_2							
V_3/V_2							
$V_3/V_2*V_1/V_2$							
$V_1/V_2*k_1/k_2$							
$V_3/V_2*k_3/k_2$							
$s_1/s_2*V_1/V_2$							
$s_3/s_2*k_3/k_2$							

4.3.6 Significant Factors for Crossflow System

For the crossflow system, the derivative curves manifest only downward drift trend with different curvature depending on the values of factors (two examples shown in **Figures 26 and 27** with different downward curvature). In the same way as the commingled system, we can fit the pressure derivative curves (two examples shown as black curves in **Figures 26** and **27**) and obtain the significant factors for the crossflow system (**Table 17**), which are more directly displayed in **Table 18**, except that we allow communication between layers in this system.

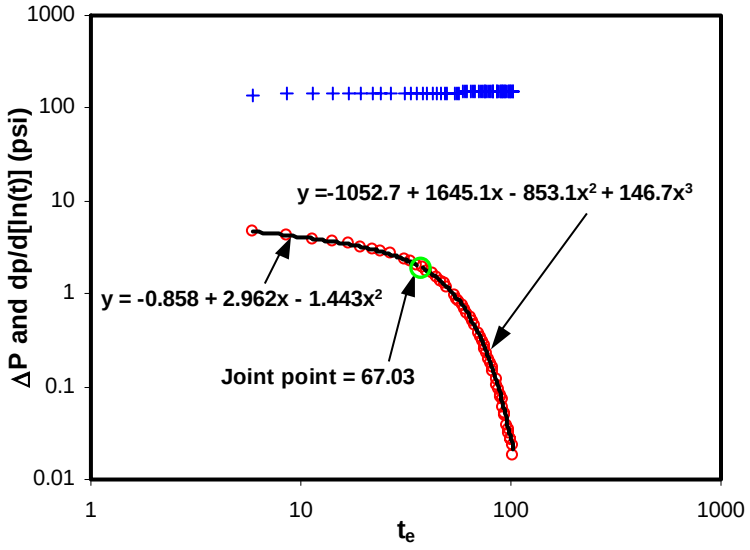

Figure 26. Example 1 for crossflow system with piecewise regression

This example corresponds to the factor combination [+1, +1, 0, -1, 0, 0, 0] (same design as example 1 in **Figure 24**), corresponding design values are [10, 10, 1, 0.2, 1, 1, 0.01] (**Table 11**).

We also choose 0.05 as the significance level. Like the commingled system, permeability influences the whole pressure behavior. However, pore volume also affects the whole pressure behavior, which is different from the commingled system, in which

pore volume only affects middle time behavior. Skin factor in combination with permeability, only significant to α_0, influence the early time behavior. This indicates that the crossflow between layers does not occur in the wellbore, but in the reservoir, which is different from the commingled system. The transition point x_j is controlled by almost all the factors. The late time behavior is mainly determined by permeability and pore volume contrast. The magnitude of crossflow, controlled by k_z/k_h, does not influence the pressure behavior.

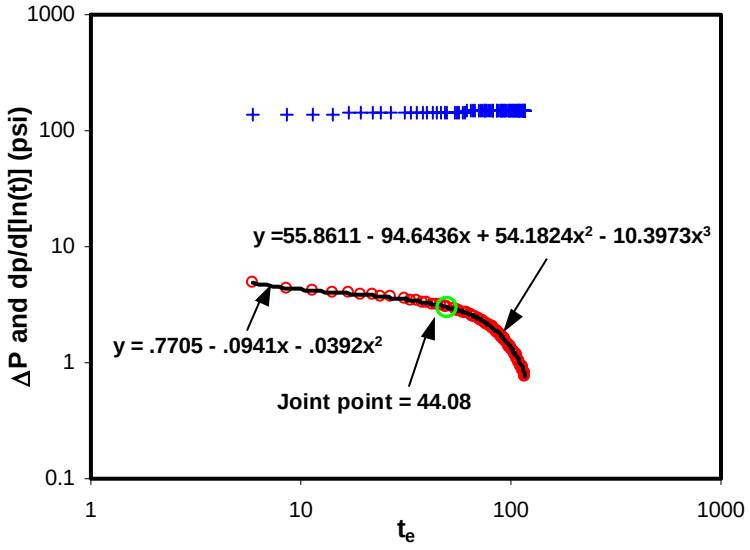

Figure 27. Example 2 for crossflow system with piecewise regression

This example corresponds to the factor combination [[+1, +1, 0, +1, 0, 0, 0] (same design as example 1 in **Figure 25**), corresponding design values are [10, 10, 1, 5, 1, 1, 0.01] (**Table 11**).

For the crossflow system, there is no phenomenon of concave-up on the Horner curve or upward-rising on the log-log derivative curve for all cases. This signifies that crossflow system is not the mechanism that causes the pressure anomaly, while the commingled system displays such phenomenon when some degree of the layer properties contrast exists. Therefore, multilayer commingled system may be the candidate.

Table 17. Significant Terms for Crossflow System

Factor or interaction	α_0	α_1	α_2	α_3	α_4	α_5	x_j
k_1/k_2	-0.5439	0.3661	-0.1693	-0.1622			7.2262
k_3/k_2	-0.4956	0.2596	-0.1161	-0.2323			6.3851
$k_1/k_2*k_1/k_2$	-0.3247						5.7534
$k_3/k_2*k_1/k_2$					-7.6945	21.9231	2.8770
$k_3/k_2*k_3/k_2$	-0.3119						3.9895
V_1/V_2				0.1508			-2.4321
V_3/V_2	0.1526	-0.2890	0.1233				-3.2350
$V_1/V_2*k_3/k_2$			0.1760				-3.8186
$V_3/V_2*k_1/k_2$	0.2028	-0.3961	0.1754		6.9271	-18.7461	-4.1770
$V_3/V_2*k_3/k_2$	0.1632				6.7147	-20.3193	
$s_1/s_2*k_1/k_2$	0.1824						
All other terms are insignificant							

Table 18. Bar Graph for Significant Terms for Crossflow System

Factor or interaction	α_0	α_1	α_2	α_3	α_4	α_5	x_j
k_1/k_2	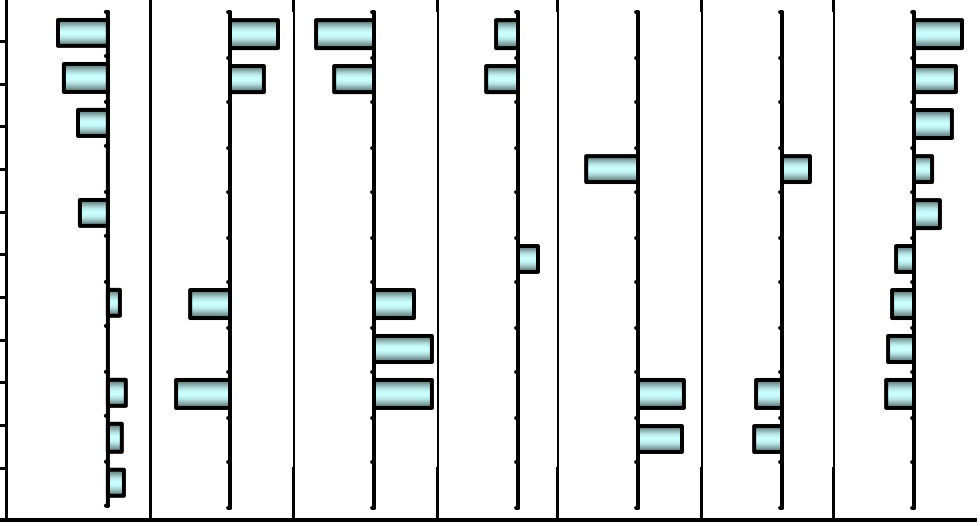						
k_3/k_2							
$k_1/k_2*k_1/k_2$							
$k_3/k_2*k_1/k_2$							
$k_3/k_2*k_3/k_2$							
V_1/V_2							
V_3/V_2							
$V_1/V_2*k_3/k_2$							
$V_3/V_2*k_1/k_2$							
$V_3/V_2*k_3/k_2$							
$s_1/s_2*k_1/k_2$							
$s_3/s_2*k_3/k_2$							

4.4 Leaky-compartment Model

We have stated above that Leaky-compartment model has similar pressure response as layered model. To analyze how factors influence these two mechanisms differently, we

design a one-layer three-compartment model, in which the three compartments have equal area (**Figure 28**) with subscript 1, 2, 3 indicating the inner, middle, outer compartment respectively. 6 factors including permeability ratios, pore volume ratios and transmissibility between compartments are included in the model. The design factors and their value ranges are shown in **Table 19**.

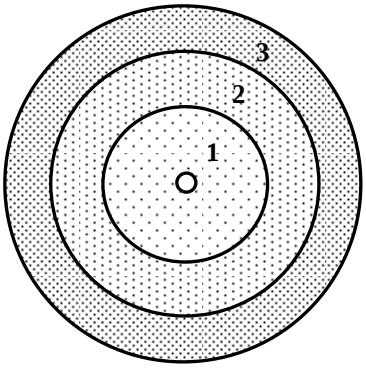

Figure 28. Schematic graph of three-compartment model

Table 19. Design Factors and Value Ranges Used for 3-Compartment Model

Design Level	k_1/k_2	k_3/k_2	V_1/V_2	V_3/V_2	T_{12}	T_{23}
-1	0.1	0.1	0.5	0.5	0.1	0.1
0	1	1	1	1	0.55	0.55
1	10	10	2	2	1	1

Table 20. Box-Behnken Design for 6 Factors

k_1/k_2	k_3/k_2	V_1/V_2	V_3/V_2	T_{12}	T_{23}
±1	±1	0	±1	0	0
0	±1	±1	0	±1	0
0	0	±1	±1	0	±1
±1	0	0	±1	±1	0
0	±1	0	0	±1	±1
±1	0	±1	0	0	±1
0	0	0	0	0	0

Again we use Box-Behnken design for the leaky-compartment model, in which 49 design points (or simulation runs) are needed (**Table 20**). After running the simulations, we can obtain the pressure response of the leaky-compartment model. The derivative curve can display either downward drift (one example shown in **Figure 29**) or upward drift trend (one example shown in **Figures 30**) depending on the properties of the zones. After fitting the derivative curves (two examples shown as the black curves in **Figures 29** and **30**), the significant factors can be obtained for the significant level of 0.05 (**Table 21**), which are more directly displayed in **Table 22**. It can be seen that the pressure behavior is mainly affected by the permeability, pore volume and their interactions of the compartment 1 and 2. The properties of compartment 3 only influence the late time behavior. The transmissibility between compartment 1 and 2 only affects the late-time pressure behavior.

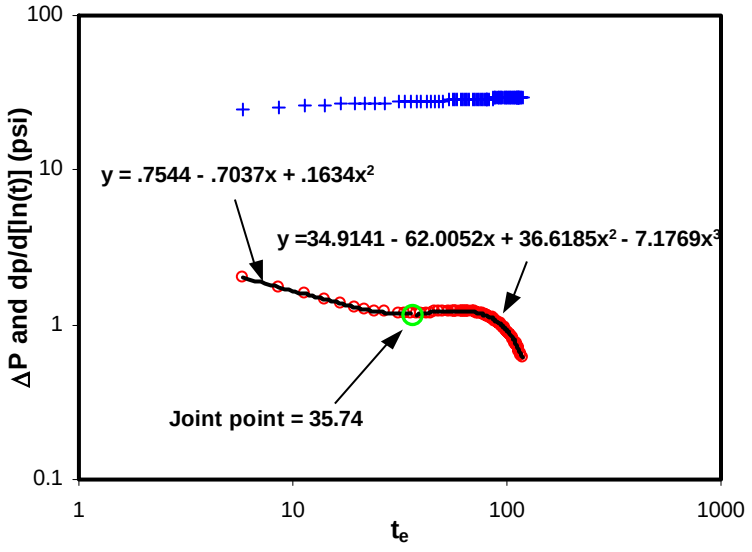

Figure 29. Example 1 for Leaky-compartment model with piecewise regression

This example corresponds to the factor combination [[+1, +1, 0, -1, 0, 0] (**Table 20**), corresponding design values are [10, 10, 1, 0.5, 0.55, 0.55] (**Table 19**).

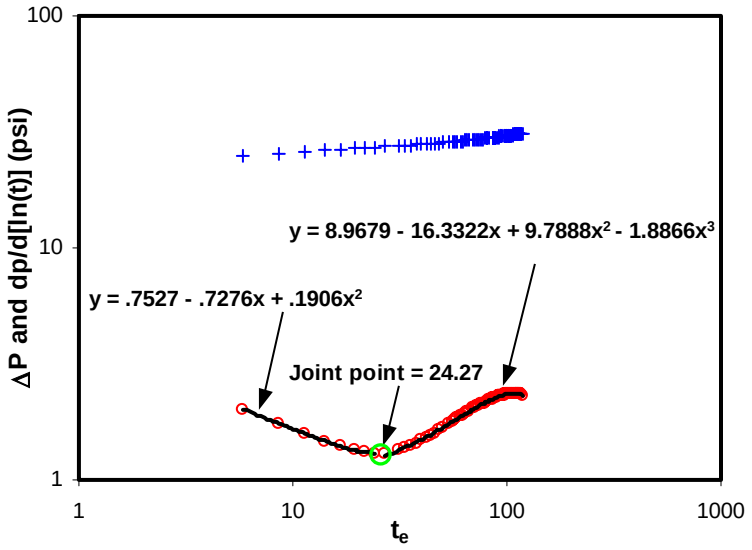

Figure 30. Example 2 for Leaky-compartment model with piecewise regression

This example corresponds to the factor combination [[+1, 0, 0, +1, -1, 0] (**Table 16**), corresponding design values are [10, 1, 1, 2, 0.1, 0.55] (**Table 15**).

Table 21. Significant Terms for Leaky-compartment Model

Factor or interaction	α_0	α_1	α_2	α_3	α_4	α_5	x_j
k_1/k_2	-1.0046			0.0589	1.0405	-1.5838	
$k_1/k_2*k_1/k_2$	0.1291	-0.2121			0.6207	-0.9574	
$k_3/k_2*k_1/k_2$					0.5228	-1.1461	
V_1/V_2	-0.0414	0.0938	-0.0535	0.0743		0.7262	
V_3/V_2						0.7160	
$V_1/V_2*V_1/V_2$						-0.9381	5.4881
$V_3/V_2*V_1/V_2$						-0.8330	
$V_1/V_2*k_1/k_2$	-0.1390	0.2995	-0.1605	0.0884	0.5625		
$V_3/V_2*k_1/k_2$						0.6482	
T_{12}						-0.4688	2.2645
$T_{12}*V_1/V_2$						0.8614	
All other terms are insignificant							

For the Leaky-compartment system, there is phenomenon of concave-up on the Horner curve or upward-rising on the log-log derivative curve for some cases with certain degree of compartment properties contrast. This signifies that Leaky-compartment model

is another mechanism that may cause the pressure anomaly like the multiplayer commingled model.

Table 22. Bar Graph for Significant Terms for Leaky-compartment System

Factor or interaction	α_0	α_1	α_2	α_3	α_4	α_5	x_j
k_1/k_2							
$k_1/k_2*k_1/k_2$							
$k_3/k_2*k_1/k_2$							
V_1/V_2							
V_3/V_2							
$V_1/V_2*V_1/V_2$							
$V_3/V_2*V_1/V_2$							
$V_1/V_2*k_1/k_2$							
$V_3/V_2*k_1/k_2$							
T_{12}							
$T_{12}*V_1/V_2$							
k_1/k_2							

CHAPTER 5. METHODS TO DISTINGUISH BETWEEN LEAKY-COMPARTMENT MODEL AND MUTILAYER COMMINGLED MODEL

Because both leaky-compartment and multilayer commingled models are possible mechanisms causing the concave-up shape on Horner plots, we need a way to distinguish these two mechanisms. Of course, there may not be pure model (only one mechanism exists in a reservoir) of these two mechanisms in reality, however, we use idealized models (or end members) for the two mechanisms for the purpose of discrimination.

5.1 Drawdown and Buildup Behavior for the Two Models

One prominent feature of the multilayer commingled model is that there is crossflow from one layer to another in the wellbore, which does not occur for the leaky-compartment model. Therefore, the behavior of drawdown and buildup may take on different feature for the two models. We designed a two-layer commingled model and a two-compartment model to investigate this. For the two-layer model, the permeability ratio is 0.1 (100 md for layer 1 and 1000 md for layer 2) and the pore volume ratio is 4 (pore volume multiplier set to 2.0 for layer 1 and 0.5 for layer 2) and the transmissibility between the two layers is set to zero to model the commingled system without formation crossflow; for the two-compartment model, the permeability ratio is also 0.1 (1000 md for inner zone and 100 md for outer zone) and the pore volume ratio is also 4 (pore volume multiplier set to 2.0 for outer zone and 0.5 for inner zone). In the compartmentalized model, the transmissibility between the two zones is reduced to model the flow barrier. After running both models, we can obtain their respective pressure response for both drawdown and buildup (**Figure 31**). For comparison, we also plotted the drawdown and buildup for a homogeneous reservoir. We can see that there is a clear flat section in both drawdown and buildup plots, which represents the transient flow

period, and there is an upward drift for drawdown and downward drift for the buildup at late time for the homogeneous model. The occurrence time of the transient period and the level of the flat section is basically the same for both drawdown and buildup. The flat section vanishes for both commingled and leaky-compartment model and there is only upward drift for both models. There is large difference between the drawdown and buildup pressure behavior for the two-layer model; the occurrence time of the inflection point on the derivative curve is quite different due to the crossflow in the wellbore from one layer to another. In contrast, there is little difference for the occurrence time and level of the inflection point between the drawdown and buildup pressure behavior for the leaky-compartment model. Because conventional well test analysis techniques assume that the wellbore is a source/sink but not a conduit (which affects the way in which boundary conditions are imposed), traditional superposition methods may not be applicable for layered reservoir pressure buildup analysis. They should still be applicable for compartmentalized reservoirs because the wellbore flux distributions remains simple.

5.2 Deconvolution for the Discrimination of the Two Models

By Duhamel's principle, we know that response from a varying boundary condition can be expressed as the convolution of the derivative of varying boundary condition and response from the constant boundary condition:

$$p_D(t_D) = \int_0^{t_D} \pi(t_D - \tau) \frac{\partial q_D(\tau)}{\partial \tau} d\tau \quad \text{.....(11)}$$

where p_D is the dimensionless pressure drop in the wellbore due to dimensionless variable sandface flowrate $q_D = q_{sf} / q_0$ and π is the dimensionless pressure drop which

would have occurred had the well been flowed at constant rate q_0, often called "influence function". In Laplace space:

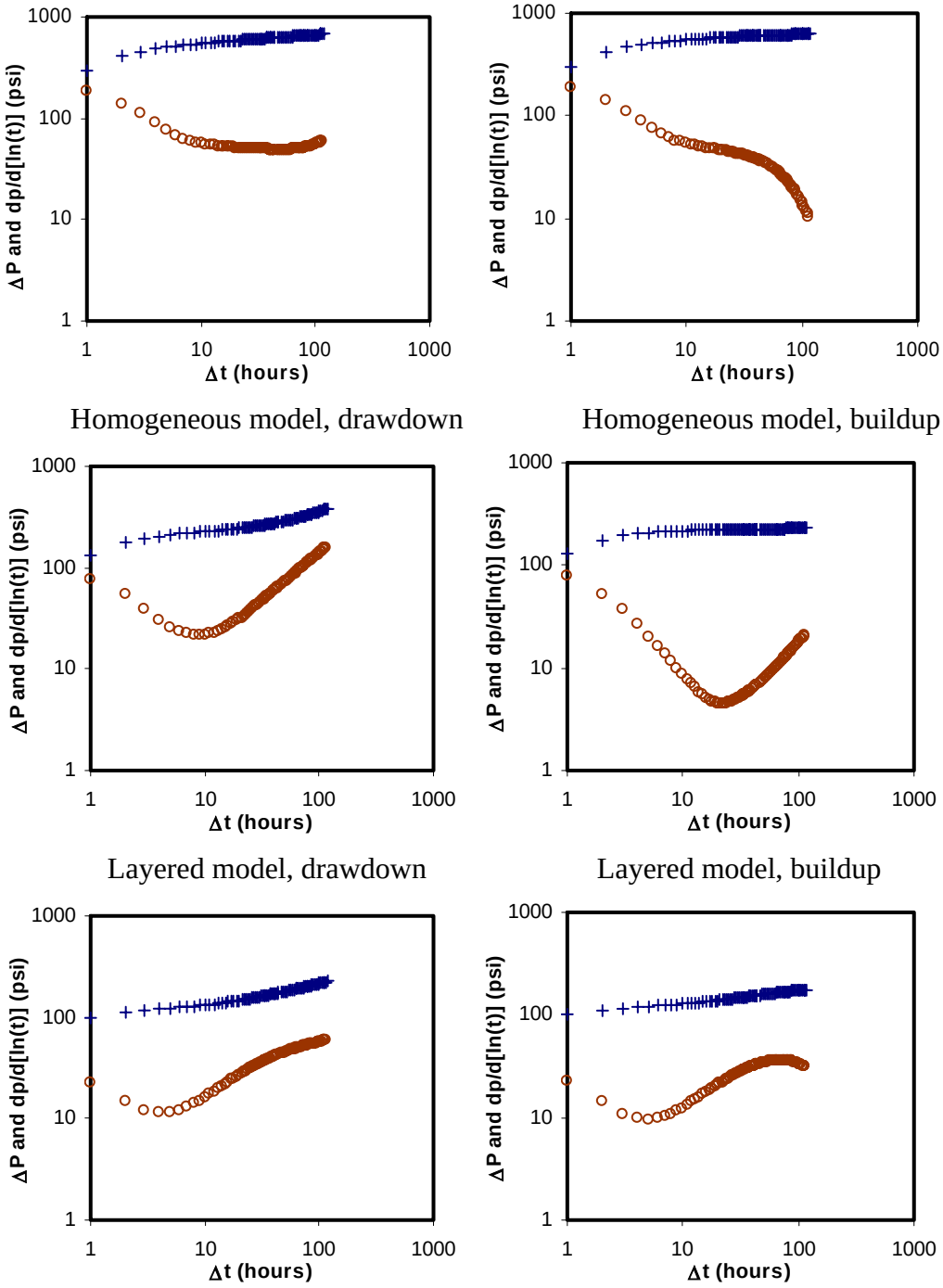

Homogeneous model, drawdown Homogeneous model, buildup

Layered model, drawdown Layered model, buildup

Leaky-compartment model, drawdown Leaky-compartment model, buildup

Figure 31. Drawdown and buildup behavior for three different models

$$P = s\Pi Q \quad \text{.....(12)}$$

where P, Q, Π are the Laplace transform of p_D, q_D, π respectively. Equation (12) can be changed to:

$$\Pi = \frac{P}{sQ} \quad \text{.....(13)}$$

If we have the measured pressure data and variable sandface flowrate, we can transform them numerically (Bourgeois and Horne, 1991) and then we can use Stehfest algorithm (Stehfest, 1970) to obtain the pressure response under constant rate.

$$\pi = L^{-1}\left(\frac{P}{sQ}\right) \quad \text{.....(14)}$$

The motivation to use deconvolution to distinguish the layered model and leaky-compartment model is that the constant-rate response calculated from Equation (14) may not conform to the actual constant-rate response from simulation since the variable flow rate we used in the deconvolution may not be the real sandface flow rate due to wellbore crossflow. For this purpose, we designed two cases for reservoir simulation. One is a 10-day constant rate drawdown, the other is 10-day variable rate simulation with multiple drawdowns and buildups for both models (**Figure 32**). The deconvolved influence function for both constant rate case and variable rate case is plotted in **Figure 33**. The influence functions for the leaky-compartment model for constant- and variable-rate

cases practically coincide, whereas the influence functions for the different rate histories are more distinct for the layered commingled model.

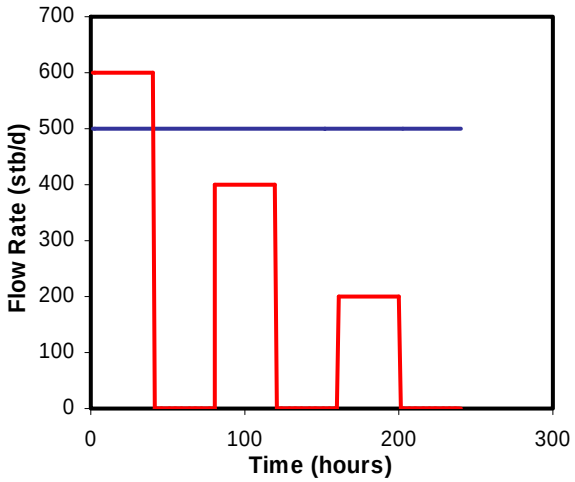

Figure 32. Constant rate and variable rate used in the deconvolution

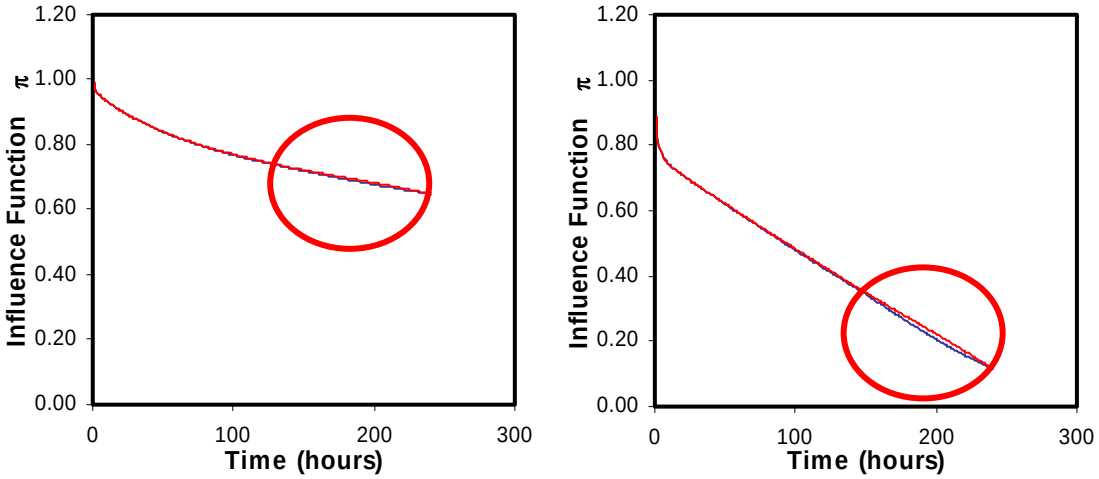

Figure 33. Deconvoluted influence function for constant and variable rate case

Leaky-compartment model is used for the left graph and layered commingled model is used for the right graph. The blue line and the red line in the plots denote the influence function for the constant rate drawdown and variable rate case respectively.

5.3 Mixed Model Behavior

Multilayered system and leaky-compartment system can coexist in the same reservoir. For example, in a turbidite reservoir, the channel-levee facies may act as compartments to a well located in the overbank. In this case, the two mechanisms may interact. To investigate how they affect each other, we designed a mixed model including both mechanisms, which has two layers and two zones (**Figure 34**).

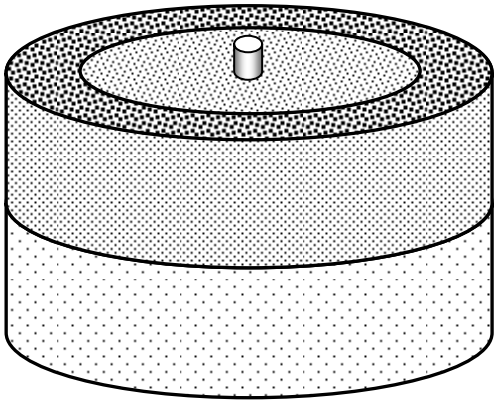

Figure 34. Schematic graph of 2-layer and 2-compartment mixed model

First, the properties of the compartments are made equal so that the mixed model becomes a pure layered model, which is the basis for the comparison to the mixed model. The Horner plot and log-log plot of the pressure response from the pure layered model are shown in **Figure 35**, which resemble the anomalous pressure behavior in Ram Powell field shown in **Figure 2**. We label permeability and pore volume of the inner zone and outer zone as k_i, k_o and V_i, V_o. By changing the properties of the two zones, we obtain different cases with different zone property contrast (**Table 23**). But we keep the layer property contrast unchanged at the same time.

Table 23. Different Compartment Property Contrast in Mixed Model

Case	k_o/k_i	V_o/V_i
1	0.1	1
2	10	1
3	1	0.25
4	1	4

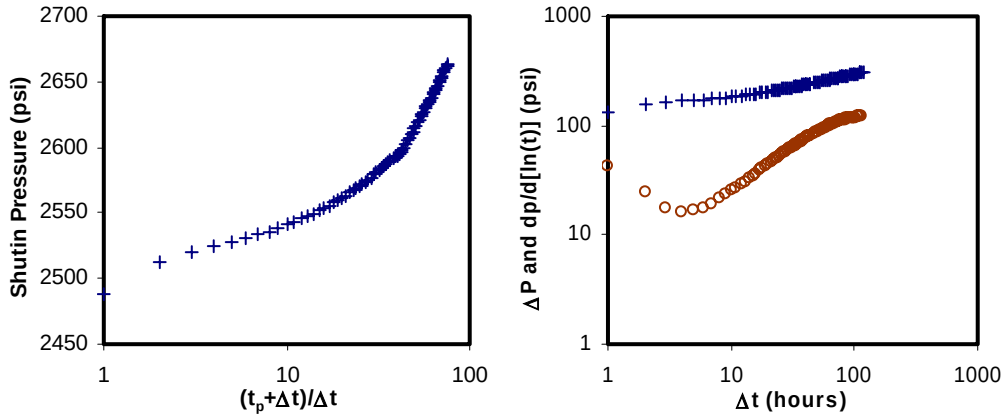

Figure 35. Horner and log-log plot of the pure layered model

After running simulation for the four cases, we compare the pressure response to that of the pure layered model (Figure 36). It can be seen that the permeability contrast between the two zones does not have much influence on the pressure behavior of the mixed model. The pore volume contrast change has some influence on the pressure behavior. The inflection point occurs later than the pure layered model, but the change is not large. This indicates the multilayer commingled effect dominates the pressure behavior, whereas the leaky compartments have little influence on the whole pressure behavior.

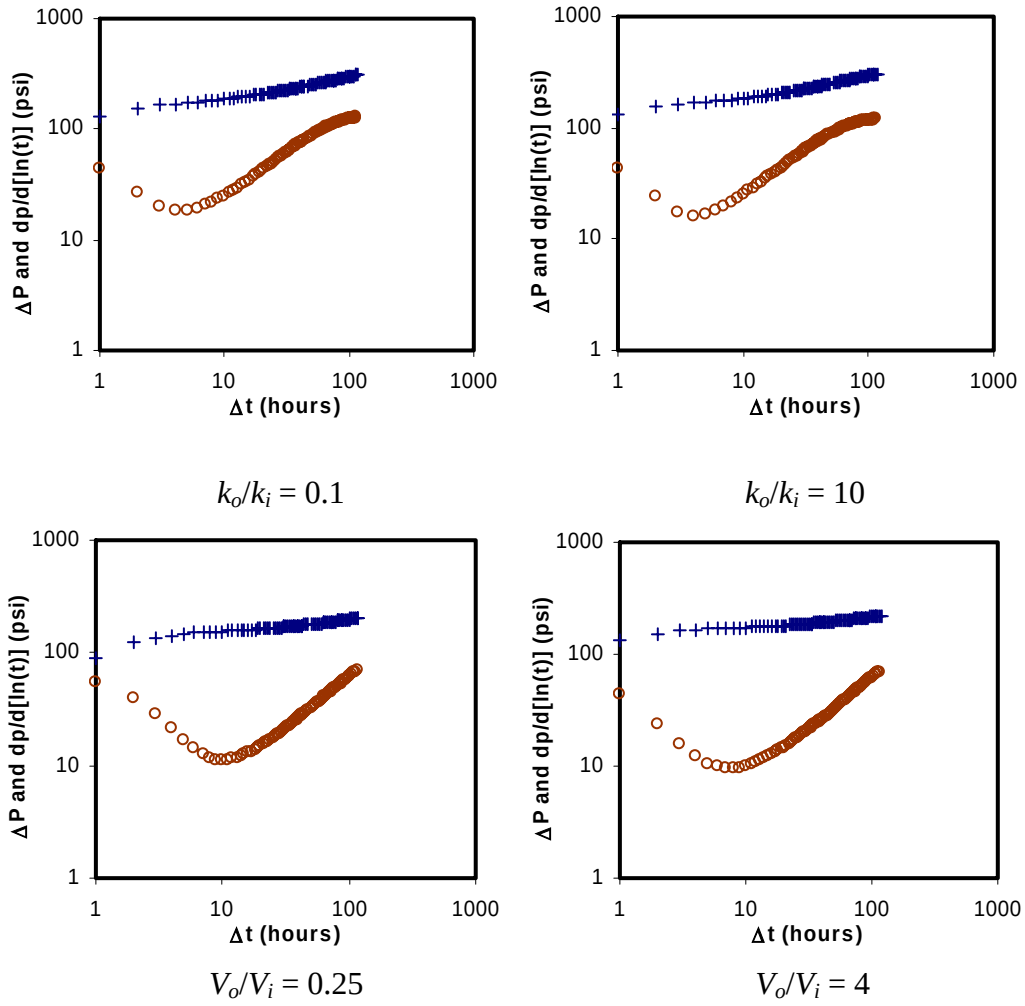

Figure 36. log-log plot for the mixed model with different compartment property

CHAPTER 6. INTERPRETATION METHODS FOR MULTILAYERED AND LEAKY-COMPARTMENT RESERVOIRS

One difficulty for the multilayered and leaky-compartment model is that the properties of the reservoir is hard to obtain even we have good well test data. Some data can be obtained from well logging or other sources, but they are often subject to uncertainty and the influence of complicated wellbore conditions. We tried to put forward a method to determine the properties of the reservoir, especially the property ratio of different layers or zones, based on the regressed polynomial on the derivative curve.

Since we have obtained the significant factors and their respective coefficient for the derivative of the multilayered and leaky-compartment model, each α is just a function of the significant factors. For example, α_1 for the regressed derivative curve for the commingled system can be expressed as a function of several factors as following equation:

$$\alpha_1 = 0.1939\frac{k_1}{k_2} + 0.1819\frac{k_3}{k_2} - 0.3046\frac{k_1}{k_2}\cdot\frac{k_3}{k_2} - 0.2919\frac{s_3}{s_2}\cdot\frac{k_3}{k_2} \quad \text{.....(15)}$$

If we have the real pressure data, we can plot a pressure derivative curve and fit a piecewise polynomial to it as stated in Chapter 4. After we have the coefficients of the polynomial, i.e., α's and the inflection point x_j, we can adjust the factor values in a spreadsheet to get a fit to all the α's and the inflection point x_j. Of course, the factor values should be constrained within the factor range when we do the experimental design because it is meaningless to extrapolate beyond the design range for a response surface model. Also, the closer to the design points the factor values are, the better the fit is. An example is shown in **Figure 37**. When the factor values are far away from the design

points, the fit is not good since non-linearity may exist for the response surface. Often there are multiple solutions (factor combinations) satisfying the same response surface model. In this case, we can look to other sources like well logging data to corroborate the factor estimation.

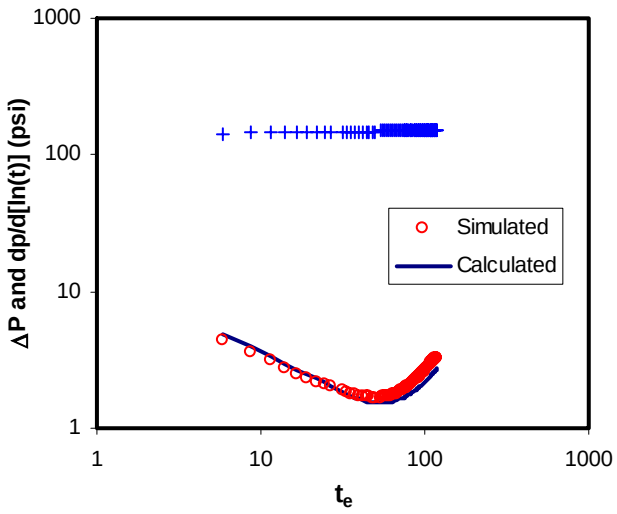

Figure 37. Example of fitting derivative curve using response surface model

Layered commingled model is used for the simulation. The selected values for the seven factors (**Table 11**) is [8, 8, 0, 0.5, 0, 0, 0], which is close to the design point [10, 10, 0, 0.2, 0, 0, 0] corresponding to the coded design level [+1, +1, 0, -1, 0, 0, 0].

Alternatively, we could change reservoir model parameters and run reservoir simulations to get a history match to the real pressure. Here we chose Well A05 in Auger oil field. Log-log plots for four different pressure buildups for the well were overlaid together. We used a three-layer commingled reservoir simulation model to simulate and match the real pressure behavior of Well A05 by adjusting permeability, pore volume and skin for each of the three layers (**Figure 38**). In the process of history matching, we used the sensitivity analysis result for 3-layer commingled model in **Table 15**. The match is good for middle time and late time. Especially the early-time upward drift trend is matched (occurred at about 1 hour). The early-time mismatch is due to the fact that we

did not take account of the near-wellbore effect like wellbore storage and non-Darcy flow in the reservoir simulation. The matched reservoir parameter values are shown in **Table 24**. Of course there are multiple realizations that would give similar pressure responses in the history match. We still need to look to other sources like well logging data for further verification for the layer properties of the model.

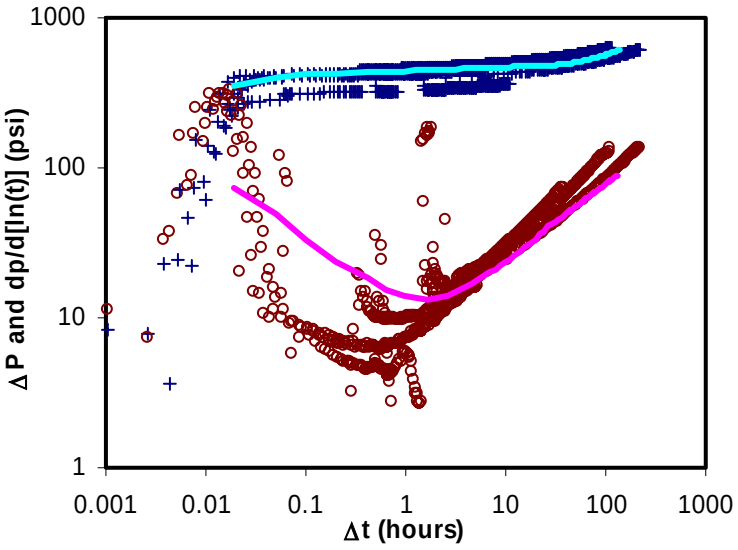

Figure 38. History match of Auger Well A05

The crosses indicate pressure difference and the circles indicate pressure derivative of the real pressure data. 3-layer commingled model is used in the history match. The lines are the simulated pressure difference and pressure derivative for the 3-layer model.

Table 24. Reservoir Parameter Values Matched for Auger Well A05

Layer	**Thickness** ft	**Permeability** md	**Area** acre	**Pore Volume Multiplier**	**Skin**
1	10	50	80	4	10
2	10	400	80	2	5
3	10	3000	80	1	0

CHAPTER 7. CONCLUSION AND DISCUSSION

In this study, the anomalous pressure behavior in the turbidite reservoirs is investigated by several mechanisms using numerical method, of which the multilayer commingled system and the leaky-compartment model turn out to be the most probable mechanisms to cause the concave-up on Horner plot or upward drift on the derivative curve of the log-log plot and the asymmetry of the pressure drawdown and buildup.

The multilayered system is first examined qualitatively by a two-layer model using some 2-level factorial experimental design. Some factors originally considered to affect the anomalous pressure behavior are excluded such as compaction and wellbore storage. Layer property (permeability, pore volume and skin) contrast is found to have the most influence on the pressure behavior. The leaky-compartment model is also examined by a two-zone model. The zone property contrast (permeability and pore volume) is proved to affect the pressure behavior. The multilayer model and leaky-compartment model can display the anomalous pressure behavior at some degree of layer property or zone property contrast. The layer flow rate analysis indicates that crossflow from one layer to another in the wellbore during shutin due to differential depletion is the cause of anomalous pressure behavior and the asymmetry of the pressure drawdown and buildup behavior. The producing time affects the degree of differential depletion, therefore, the buildup behavior is strongly influenced by the producing time. However, crossflow between the layers in the formation would eliminate above phenomena and make the pressure behavior look like a single-layer reservoir.

The multilayered system is further investigated quantitatively by a three-layer model representing low, medium and high properties of a reservoir. 3-level Box-Behnken

design and a non-linear piecewise regression procedure are used to analyze the sensitive factors to the shape of derivative curve for multilayered model and leaky-compartment model. Again, layer or zone property contrasts contribute to the shape change of the derivative curve. The conclusions drawn from the two-layer model are further verified. In addition, we can obtain factor value estimates from matching the derivative curve by using the reduced models (only contains significant factors) that describe the relationship between α's and the factors (or factor interactions)**.** When there are multiple solutions other, data sources should be consulted to determine the reservoir parameters.

The pressure responses from a multilayer commingled system and leaky-compartment system are sometimes similar. Asymmetry of the pressure drawdown and buildup behavior due to crossflow in the wellbore is a prominent feature for the multilayer commingled system, which can be used to distinguish the two systems. Numerical deconvolution is also tried to obtain influence functions for discriminating the two systems. The multilayer commingled system is proved to be the dominant mechanism if both systems coexist in the same reservoir.

The multilayered system actually can produce pressure behavior of many types of reservoir from homogeneous to double porosity. So layered reservoirs may not produce the anomalous pressure behavior as seen in this study. When we encounter homogeneous, double-permeability or double-porosity pressure response, we cannot exclude the possibility of a layered reservoir. Well testing interpretation in this situation would often be based on the wrong models and the interpreted reservoir parameters would be problematic. Geological evidence of appropriate reservoir models is important for the well testing interpretation.

REFERENCES

Bourdet, D.: "Pressure Behavior of Layered Reservoirs with Crossflow," paper SPE 13628 presented at the 1985 SPE California Regional Meering, Bakersfield, Mar. 27-29.

Bourgeois, M. and Horne, R.N.: "Well Test Model Recognition using Laplace Space Type Curves," paper SPE 22682 presented at the 66th SPE Annual Technical Conference and Exhibition, Dallas, TX, Oct. 6-9, 1991.

Box, George E.P. and Draper N.R.: *Empirical Model-Building and Response Surface*, New York: Wiley (1987), 669 p.

Bramlett, K.W. and Craig, P.A.: "Core Characterization of Slope-channel and channel-levee reservoirs in Ram Powell Field, Gulf of Mexico", Ram Powell Project Report (2002), Shell E & P Company, New Orleans, LA.

Cobb, W.M., Ramey, H.J. Jr. and Miller, F.G.: "Well-Test Analysis for Wells Producing Commingled Zones," *JPT* (Jan. 1972) 27-37.

De Kock, A.J., Johnson, T.J., Hagiwara, T., Zea, H.A. and Santa, F.: "Gulf of Mexico subsidence Monitoring Project With a New Formation-Compaction Monitoring Tool," *SPE Drilling & Completion* (December 1998), p. 223-230.

Earlougher, R.C., Kersch, K.M., and Kunzman, W.J.: "Some Characteristics of Pressure Buildup Behavior in Bounded Multiple-Layered Reservoirs Without Crossflow," *JPT* (Oct. 1974) 1178-85.

Ehlig-Economides, C.A., Joseph, J.: "A New Test for Determination of Individual Layer Properties in a Multilayered Reservoir," *SPE Formation Evaluation* (Sept. 1987) 261-83.

Fair, P.S. and Simmons, J.F.: "Novel Well Testing Applications of Laplace Transform Deconvolution," paper SPE 24716 presented at the 67th SPE Annual Technical Conference and Exhibition, Washington, DC, Oct. 4-7, 1992.

Fair, P.S., Kikani, J. and White, C.D.: "Modeling high-angle wells in laminated pay reservoirs," Soc. of Petroleum Engineers Reservoir Evaluation and Engineering J. (SPEREE) (February 1999), v. 2 no. 1, p. 46-52.

Fox, M.F. Chedburn, A.C.S. and Stewart, G.: "Simple Characterization of Communication between Rservoir Regions," paper SPE 18360 presented at the 1988 SPE European Petroleum Conference, London, UK, Oct. 16-19.

Gao, C. and Deans, H.A.: "Single-Phase Flow in a Two-Layer Reservoir with Significant Crossflow-Pressure Drawdown and Buildup Behavior When Both Layers are Completed at a Single Well," paper SPE 11874 available at SPE, Richardson, TX, 1983.

GeoQuest, Schlumberger, *ECLIPSE 100 Reference Manual* (2002A).

Horne, R.N.: "Uncertainty in Well Test Interpretation," paper SPE 27972 presented at the University of Tulsa Centennial Petroleum Engineering Symposium, Tulsa, OK, Aug. 19-31, 1994.

Junkin, J.E., Sippel, M.A., Collins, R.E., and Lord, M.E.: "Well Performance Evidence for Compartmented Geometry of Oil and Gas Rervervoirs," paper SPE 24356 presented at the SPE Rocky Mountain Regional Meeting, Casper, WM, Oct. 1-4, 2000.

Kappa Engineering Company, *Saphir v3.01 Online Documentation*, 2002.

Kikani, J., Fair, P.S. and Hite R.H.: "Pitfalls in Pressure Gauge Performance," paper SPE 30613 presented at the SPE Annual Technical Conference and Exhibition, Dallas, TX, Oct. 22-25, 1995.

Lefkovits, H.C., Hazebroek, P., Allen, E.E. and Matthews, C.S.: "A Study of the Behavior of Bounded Reservoirs Composed of Stratified Layers," *Soc. Pet. Eng. J.* (March 1961) 43-58.

Myers, R.H. and Montegomery, D.C.: *Response Surface Methodology: Process and Product optimization Using Designed Experiments*, New York: Wiley (1995), 700 p.

Ostermeier, R.M.: "Compaction Effects on Porosity and Permeability: Deepwater Gulf of Mexico Turbidites," *JPT* (February 2001), p. 68-74.

Petro, D.R., Chu, W.C., Burk, M.K. and Rogers, B.A.: "Benefits of Pressure Transient Testing in Evaluating Compaction Effects: Gulf of Mexico Deepwater Turbidite Sands," SPE 38938, SPE Ann. Tech. Conference and Exhibition, San Antonio, Texas, October 5-8, 1997.

Pettingill, H.S.: "Worldwide turbidite Exploration and Production: A Globally Immature Play with Opportunities in Stratigraphic Traps," paper SPE 49245 presented at the SPE Annual Technical Conference and Exhibition, New Orleans, Louisiana, September 27-30, 1998.

Rahman, N.M.A. and Ambastha, A.K.: "A Generalized Transient-Pressure Model for Areally-Compartmentalized Reservoirs," paper SPE 37340 presented at the 1996 SPE Eastern Regional Meeting, Columbus, Ohio, Oct. 23-25, 1996.

Rahman, N.M.A. and Ambastha, A.K.: "A Generalized 3D Analytical Model for Transient Flow in Compartmentalized Reservoirs," paper SPE 38675 presented at the 72nd SPE Annual Technical Conference and Exhibition, San Antonio, TX, Oct. 5-8, 1997.

Raghavan, R., Topaloglu, H.N., Cobb, W.M., Ramey, H.J. Jr.: "Well-Test Analysis for Wells Producing From Two Commingled Zones of Unequal Thickness," *JPT* (Sept. 1974) 1035-40.

Romboutsos, A. and Stewart, G.: "A Direct Deconvolution or Convolution Algorithm for Well Test Analysis," paper SPE 18157 presented at the 63rd SPE Annual Technical Conference and Exhibition, Houston, TX, Oct. 2-5, 1988.

Russell, D.G. and Prats, M.: "The Practical Aspects of Interlayer Crossflow," *JPT* (June 1962) 589-92.

Sabet, M.A.: Well Test Analysis, Gulf Publishing Company (1991), 460 p.

SAS Institute, *SAS/STAT User's Guide*, SAS OnlineDoc, version 8, 1999.

Stehfest, H.: "Numerical Inversion of Laplace Transforms," *Communication of the ACM*, Jan. 1970, Vol. 13, No.1, 47-49.

Stewart, G. and Whaballa, A.E.: "Pressure Behavior of Compartmentalized Reservoirs," paper SPE 19779 presented at the 64th SPE Annual Technical Conference and Exhibition, San Antonio, TX, Oct. 8-11, 1989.

Streltsova, T.D.: Well Testing in Heterogeneous Formations, An Exxon Monograph, John Wiley & Sons (1988), 413 p.

Tariq, S.M. and Ramey, H.J. Jr.: "Drawdown Behavior of a Well With Storage and Skin Effect Communicating With Layers of Different Radii and Other Characteristics," paper SPE 7453 presented at the SPE Annual Technical Conference and Exhibition, Houston, TX, Oct. 1-3, 1978.

White, C.D., Bradburn, F.R., Brown, R.L., and Thieme, M.A.: "Reservoir potential of thin-bedded turbidites, Prospect Tahoe," paper SPE 24875 presented at the 67th SPE Annual Technical Conference and Exhibition, Washington, DC, October 4-7, 1992.

White, C.D., Willis, B.J., Narayanan, K., and Dutton, S.P.: "Identifying controls on reservoir behavior using designed simulations," paper SPE 62971 presented at the SPE Annual Technical Conference and Exhibition, Dallas, TX, Oct. 1-4, 2000.

VITA

Feng Wang was born in Xixia County, Henan Province, China, on May 7th, 1972. He entered the University of Petroleum (East China) in September 1989 where he obtained the degree of Bachelor of Science in Petroleum Engineering in July 1993. After graduation, he worked in the Research Institute of China Offshore Oil Bohai Corporation. Then he was admitted to the Graduate School of Louisiana State University in August 1999 for the master's program in the Craft & Hawkins Department of Petroleum Engineering and he obtained the degree of Master of Science in Petroleum Engineering in August 2001. After that, he continued his study for a higher degree and he will receive the degree of Doctor of Philosophy in petroleum engineering in May 2005. Simultaneously, he will obtain the degree of Master of Applied Statistics from the Department of Experimental Statistics.